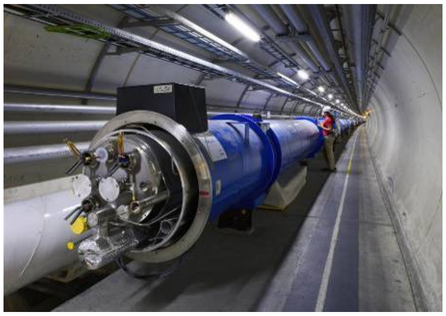

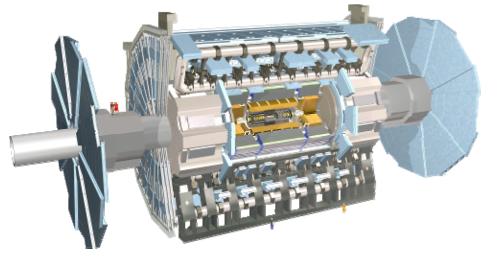

Energy dump of the ATLAS superconducting system

Simulations of electrical and thermal behaviour of the magnet system at slow- and fast-dump

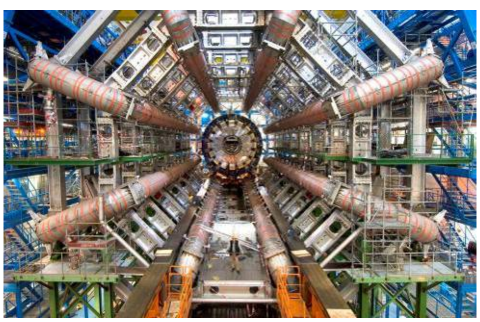

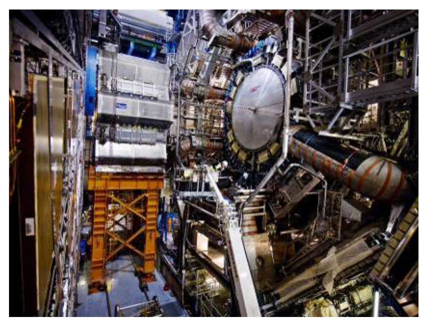

CERN-THESIS-2008-046
11/06/2008

Graduation report

Date: 11 June 2008
Name: Martijn van Beek

Fontys Hogescholen
Rachelsmolen 1
5612 MA Eindhoven
The Netherlands

Supervisor: A. Graat

CERN
385, Route de Meyrin
1211 Geneva 23
Switzerland

Supervisor: A. Dudarev

Energy dump of the ATLAS superconducting system

Simulations of electrical and thermal behaviour of magnet system at slow- and fast dump

Graduation report - spring 2008

Date: 11 June 2008
Name: Martijn van Beek

Fontys Hogeschool
Supervisor: A. Graat

CERN
Supervisor: A. Dudarev

Summary

During the slow dump (discharge) of the Barrel Toroidal (superconducting) magnet of the ATLAS detector, the control system gave an alarm that the differences between the voltages over the conductors were too high. The alarm was not due to any danger, because of some sort of phenomenon observed in the first few seconds after start of the discharge.

A possible explanation of the differences of the coil voltages is that the changing current through the conductors may cause induced currents in the coil casing around. The goal was to make a simulation of the electrical behaviour of the magnet system during a slow dump. In this way, an explanation can be found for the start phenomenon of the slow dump of the Barrel Toroid.

Some extra analyses on the measurements were performed to describe the energy dissipation during a fast dump. This is done by calculating the resistance of the coils during the dump. With the maximum resistance, the maximum temperature can be estimated, which says something about the enthalpy of the material. There is also found something about the RRR of the conductor and its relation to the properties of the quench.

The results of the simulation of the Barrel Toroid as one coil were as expected. The simulation is correct and precise enough to reproduce the measurements. This simulation was extended to a simulation of the eight coils separately. The result was that a change up to 4% in the resistance of the coil casing can be the cause of the difference in the coil voltages in the beginning of the slow dump.

The calculations of the energy dissipation during a fast dump of the BT showed that 73% of the energy was stored in the conductor. The aluminium in the conductor stored 64% of this energy and 17% was stored in the isolation, the casing and the dump unit. Not for all the parts of the magnet the change in enthalpy is calculated. An undefined 10% of the energy is also due to the inaccuracy of the calculations.

By analysing a fast dump measurement of the Barrel Toroid, it appeared that a double pancake with a relative low RRR has a relatively higher maximum temperature after the dump, as expected. For both ECTs, the RRR is measured and calculated for all the double pancakes. The ECTs showed that a double pancake quenched later, when it has a higher value for the RRR with respect to other double pancakes.

Foreword

CERN is a well known institute in the world of fundamental physics. I am interested in that subject and so it would be nice to go to CERN.

For my traineeship I did not do the application, because how could I possibly be good enough for CERN? For my graduation I though: “Why not? Who knows what could happen.”. And so I filled in the form, four days before the deadline.

A few weeks and mails later I got the message that I was selected to go to CERN. I needed the rest of the day to realise that I was going to Geneva in two months, for six months.

This is my graduation report, which describes a part of the work I did: many analyses and calculations about resistances, heat loads, temperature, RRR, inductances, energies and so on. It was all about the superconducting magnet system of the detector ATLAS, the biggest detector of the new LHC. The machine is so big and so complex, and all that, for those smallest things we know.

Looking back, I did not do anything about particle physics, except for two seminars I visited. One was about gravitational waves and the other was about the possibility of black holes and other holes in the LHC. (I knew I was not going to work on those things.)

It took me a little while to find my routine at CERN and in Geneva. It was nice to see when people where surprised by my results. We all gained more understading about the magnet system because of the results of the analyses.

Table of content

Summary III
Foreword IV
Table of content V
1 Introduction 1
2 General information 2
2.1 CERN 2
2.2 LHC 3
2.3 ATLAS 4
3 Technical information 7
3.1 Magnet system 7
3.2 Control system 10
3.3 Electrical circuit 11
3.4 Simulation 15
4 Simulation of one coil 16
4.1 Theory 16
4.1.1 Definitions 16
4.1.2 Formulas 17
4.2 Results 19
4.3 Conclusion 23
5 Simulation of eight coils 24
5.1 Theory 24
5.1.1 Definitions 24
5.1.2 Formulas 25
5.2 Results 27
5.3 Conclusion 32
6 Energy distribution 33
6.1 Method 33
6.2 Calculations 35
6.3 Results 45
7 Residual resistance ratio 47
7.1 Theory 47
7.2 Methods 48
7.2.1 Fast dump 48
7.2.2 Resistance measurement 49
7.3 Measurements 49
7.3.1 Barrel Toroid 49
7.3.2 End-Cap Toroids 51
7.4 Conclusion 55
8 Conclusion 56
9 References 57

Appendix 58
A Overview properties magnet system ATLAS 58
A.1 General properties 58
A.2 Electrical properties Barrel Toroid 58
B Simulation of one coil 59
C Simulation of eight coils 64
D Editing of data of fast dump 70
E Material properties 72
E.1 Aluminium 72
E.2 Copper 73
E.3 Insulation (Fiberglas-epoxy G-10) 73

1 Introduction

In the chapters 2 and 3 general and technical information about CERN and the assignment will be given. In the assignment description that follows, is assumed that this information is known.

During the slow dump of the Barrel Toroid, the control system gave an alarm that the differences between the voltages over the conductors were too high and the fast dump had to be started. The alarm was not due to any danger, because of some sort of phenomenon observed in the first few seconds after start of the discharge.

A possible explanation of the differences of the coil voltages is that the changing current through the conductors may cause induced currents in the coil casing around.

The goal is to make simulations of the electrical behaviour of the magnet system during a slow dump. In this way, an explanation can be found for the start phenomenon of the slow dump of the Barrel Toroidal magnet of the ATLAS detector.

Two simulations are made. The first one is a simulation of the Barrel Toroid presented as one coil with one secondary coil, which represents the casing of the Barrel Toroid. This simulation is for the understanding of the circuit and its behaviour. After this, the simulation is extended to a simulation of eight coils with each an induced coil. The goal of this second simulation is to reproduce the measurements.

Some extra analyses on the measurements are performed to describe the energy dissipation at the fast dump. During the fast dump, energy is dissipated within the magnet. There is investigated how much energy goes into the different part of the magnets. There is also found something about the RRR of the conductor and its relation to the properties of the quench.

The two simulations can be found in the chapters 4 and 5. In the chapters 6 and 7 the energy distribution and the RRR calculations are presented. In chapter 8 an overall conclusion is given. In this report, a number between brackets, like (1) for example, refers to a source, listed in chapter 9. After this last chapter one can find the appendices.

2 General information

In this chapter[1] CERN, the particle accelerator LHC and about one of its detectors, ATLAS, are presented.

2.1 CERN

CERN, the European Organization for Nuclear Research, is one of the world's largest and most respected centres for scientific research. Its business is fundamental physics, finding out what the universe is made of and how it works. At CERN, the world's largest and most complex scientific instruments are used to study the fundamental particles. By studying what happens when these particles collide, physicists learn about the laws of nature.

The instruments used at CERN are particle accelerators and detectors. Accelerators boost beams of particles to high energies before they are made to collide with each other or with stationary targets. Detectors observe and record the results of these collisions.

CERN is run by 20 European Member States, but many non-European countries are also involved in different ways. The Netherlands is one of the current Member States. Member States have special duties and privileges. They make a contribution to the capital and operating costs of CERN's programmes. They are represented in the council, responsible for all important decisions about the organization and its activities.

CERN employs just around 2500 people. The laboratory's scientific and technical staff designs and builds the particle accelerators and ensures their smooth operation. They also help prepare, run, analyse and interpret the data from complex scientific experiments. Some 8000 visiting scientists, half of the world's particle physicists, come to CERN for their research. They represent 580 universities and 85 nationalities.

Most people do not know that in 1990, CERN scientist Tim Berners-Lee invented the World Wide Web. It was a distributed information system for the laboratory. Now the Web has been developed and it has changed the way we live.

In 1983, CERN announced the discovery of the W and Z particles, carriers of the weak interaction between particles. The experimental results confirmed the unification of weak and electromagnetic forces, a theory of the Standard Model. The discovery was awarded with the Nobel Prize in physics only a year after, in 1984. Also in 1952, 1976, 1988 and 1992 physicists related to CERN, received the Novel prize for physics.

2.2 LHC

The Large Hadron Collider (LHC) will be the world's largest and most powerful particle accelerator. It mainly consists of a 27 km ring of superconducting magnets, about 100 m underground. A part of the LHC can be seen in figure 2.1. Hadrons are made up of 3 quarks and/or antiquarks or a pair of a quark and an antiquark. The hadrons that will be used in the LHC are protons. For another program, lead ions will be accelerated.

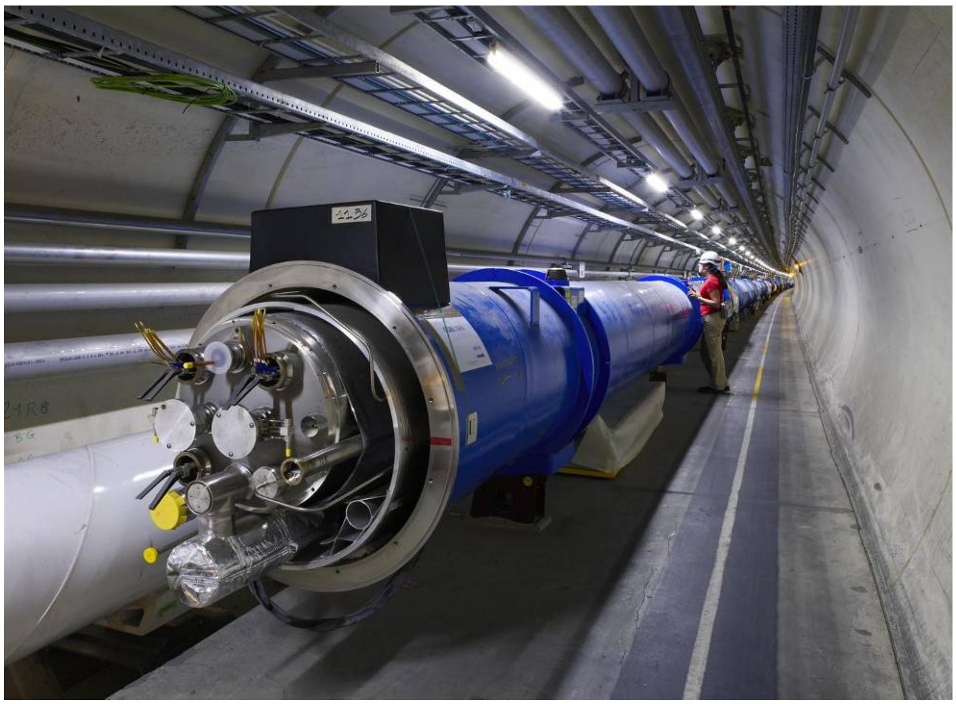

Figure 2.1: *A part of the LHC.*

The hadrons are guided around the accelerator ring by a strong magnetic field, achieved using superconducting electromagnets. These are built from coils of a special electric cable that operates in a superconducting state. In this state, the cable conducts electricity without resistance or loss of energy. This requires cooling the magnets to about 2 K.

At full power, trillions of protons will race around the LHC accelerator ring 11 245 times a second, travelling at 99.9999991% the speed of light. Two beams of protons will travel each at a maximum energy of 7 TeV. All together, some 600 million collisions will take place every second. To avoid colliding with gas molecules inside the accelerator, the beams of particles travel in an ultra-high vacuum. The internal pressure of the LHC is 10^{-13} atm.

For decades, the Standard Model of particle physics has served physicists well as a means of understanding the fundamental laws of Nature, but it does not tell the whole story. Only experimental data using the higher energies reached by the LHC can push knowledge forward.

All the controls for the accelerator, its services and technical infrastructure are housed under one roof at the CERN Control Centre. From here, the beams inside the LHC will be made to collide at four locations around the accelerator ring, corresponding to the positions of the particle detectors. When the LHC starts operating, it will produce roughly 15 petabytes (15 million gigabytes) of data per year.

There has been investigated if the LHC would be safe. An example is the generation of black holes in the LHC. Massive black holes are created in the universe by the collapse of massive stars, which contain enormous amounts of gravitational energy that pulls in surrounding matter. Some physicists suggest that microscopic black holes could be produced in the LHC. However, these would only be created with the energies of the colliding particles (equivalent to the energies of mosquitoes), so no black holes produced inside the LHC could pull in surrounding matter.

The six experiments at the LHC are all run by international collaborations. Each experiment is characterised by its unique particle detector. The two largest experiments, ATLAS and CMS, are designed to investigate the largest range of physics possible. Having two independently designed detectors is vital for cross-confirmation of any new discoveries made.

To sample and record the results of up to 600 million collisions per second, physicists and engineers have built enormous devices that measure particles with incredible precision. The LHC's detectors have electronic trigger systems that precisely measure the passage time of a particle to accuracies in the region of a few billionths of a second. The trigger system also registers the location of the particles to millionths of a metre. This incredibly quick and precise response is essential for ensuring that the particle, recorded in different layers of a detector, is one and the same.

2.3 ATLAS

ATLAS, A Toroidal LHC ApparatuS, is the largest volume particle detector ever constructed. It is 46 m long, 25 m high and 25 m wide. Its total weight is 7.000.000 kg. A drawing is shown in the figure underneath.

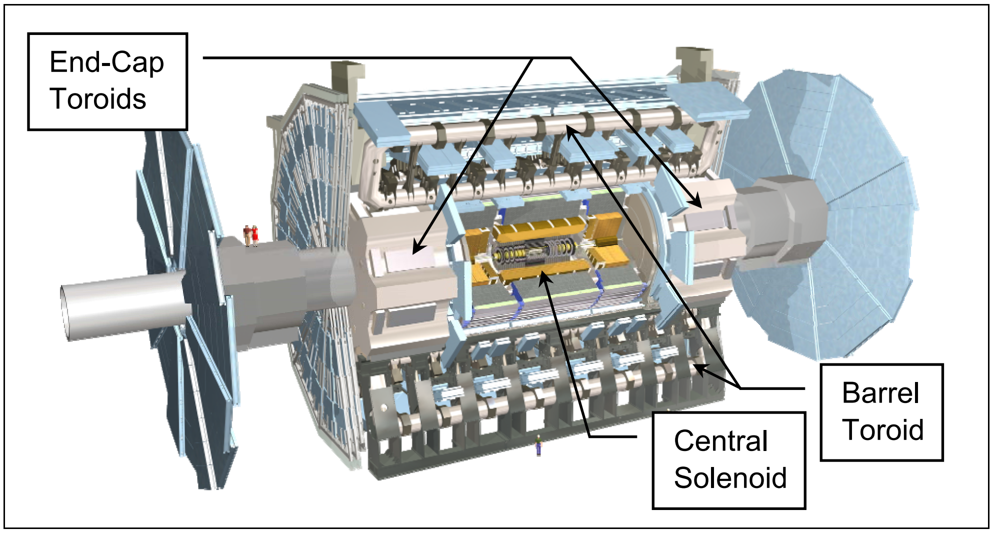

Figure 2.2: *Drawing of ATLAS.*

It will be used in the search for the Higgs boson, extra dimensions and particles that could make up dark matter. ATLAS will record sets of measurements on the particles created in the collisions – their path, energy and their identity.

The main feature of the ATLAS detector is its enormous doughnut-shaped magnet system. The magnet system consists of four parts: the Central Solenoid, the Barrel Toroid and two End-Cap Toroids. The different parts are shown in the drawing of figure 2.2. Figure 2.3 shows all the magnets without the rest of the detector.

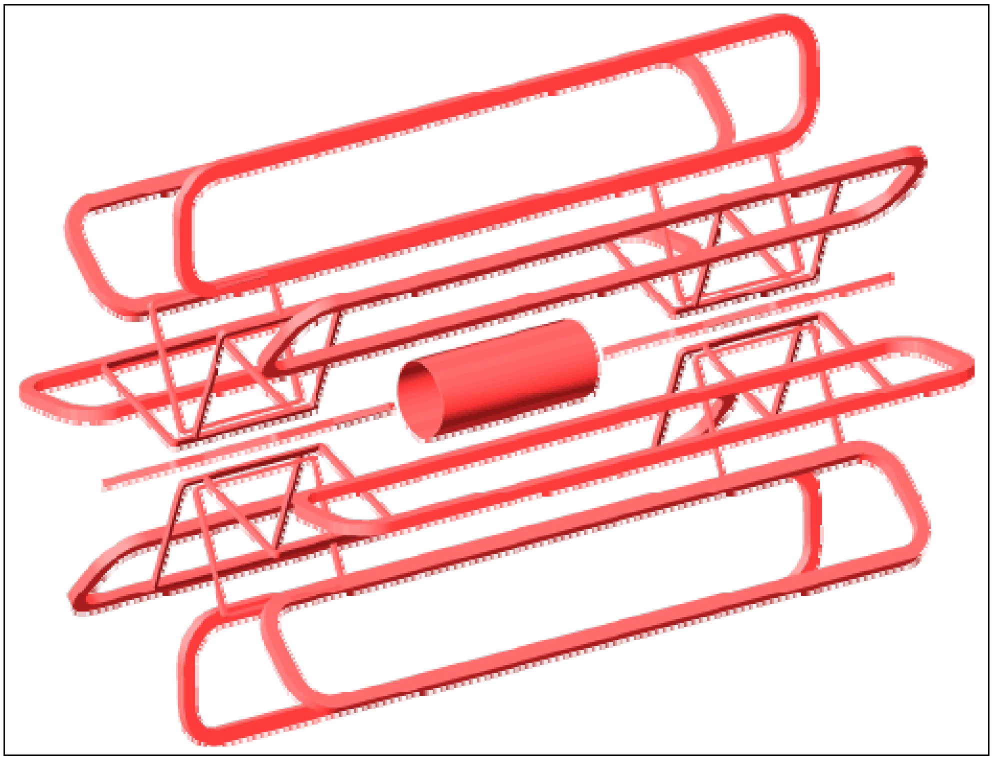

Figure 2.3: *Drawing of magnet system.*

3 Technical information

In this chapter more information about the magnet system of the ATLAS is given. One can find information about the design of the magnets, the control system and the electrical scheme.

3.1 Magnet system

The magnet system of the ATLAS detector consists of four parts: the Central Solenoid (CS), the Barrel Toroid (BT) and two End-Cap Toroids (ECTs). This report will be about the Barrel Toroid and the End-Cap Toroids. An overview of some general properties of these toroids can be found in appendix A.1(2).

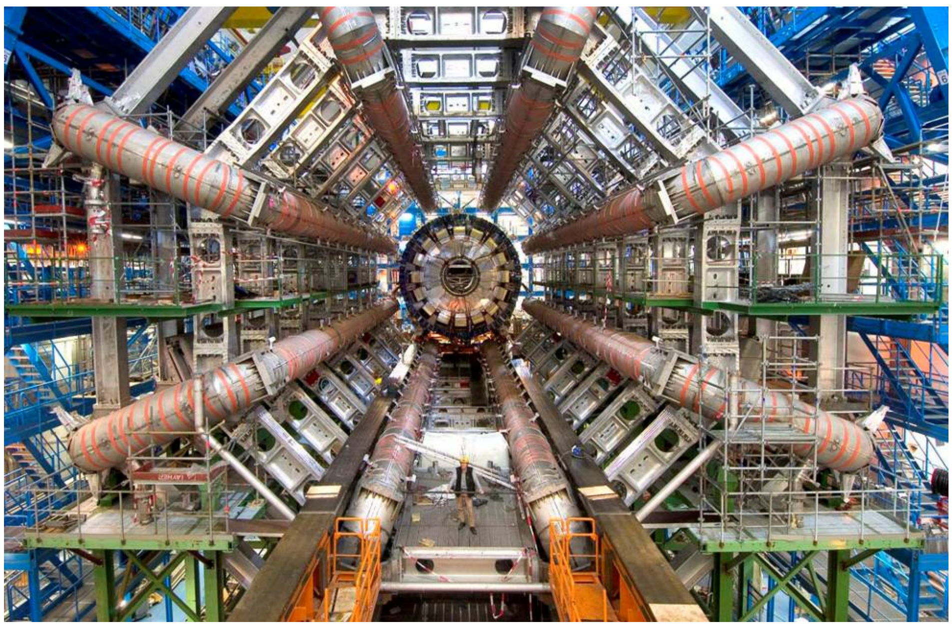

Figure 3.1: *Barrel Toroid consisting of eight coils.*

On the photo above, the Barrel toroid can be seen. It consists of eight 25 m long superconducting coils are connected in serie. 20.500 A of operating current induce a magnetic field in a very large volume of the ATLAS detector with a peak value of 3.9 T. For the Barrel Toroid the magnetic field in the centre of the detector is shown in figure 3.2. The energy stored in the BT is 1080 MJ. By the use of liquid Helium the coils are kept cold at 4.5 K.

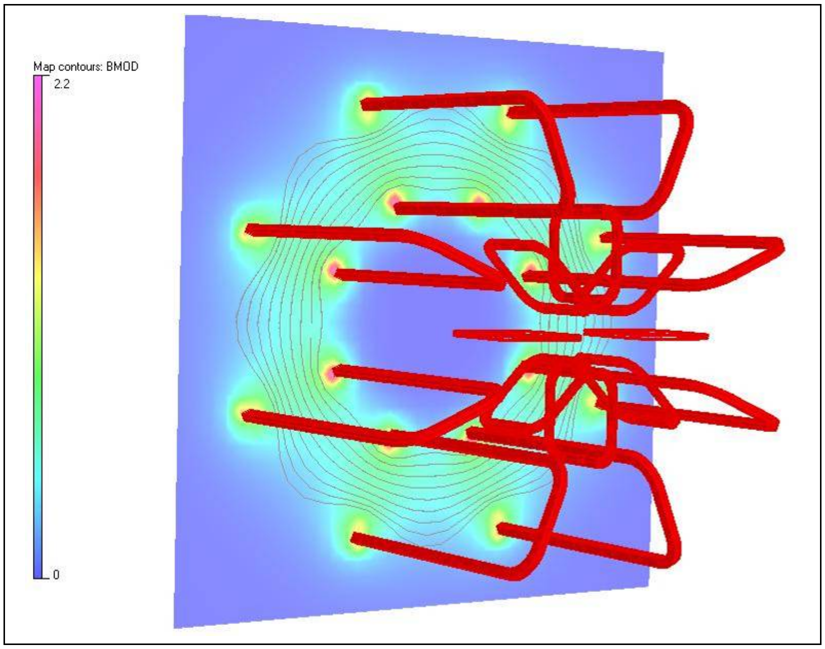

Figure 3.2: *Magnetic field of Barrel Toroid.*

Each coil consists of two double pancakes. These pancakes are placed in a coil casing. In figure 3.3 one can find a drawing of the cross section of a coil of the BT. In the drawing the four single pancakes are clearly shown.

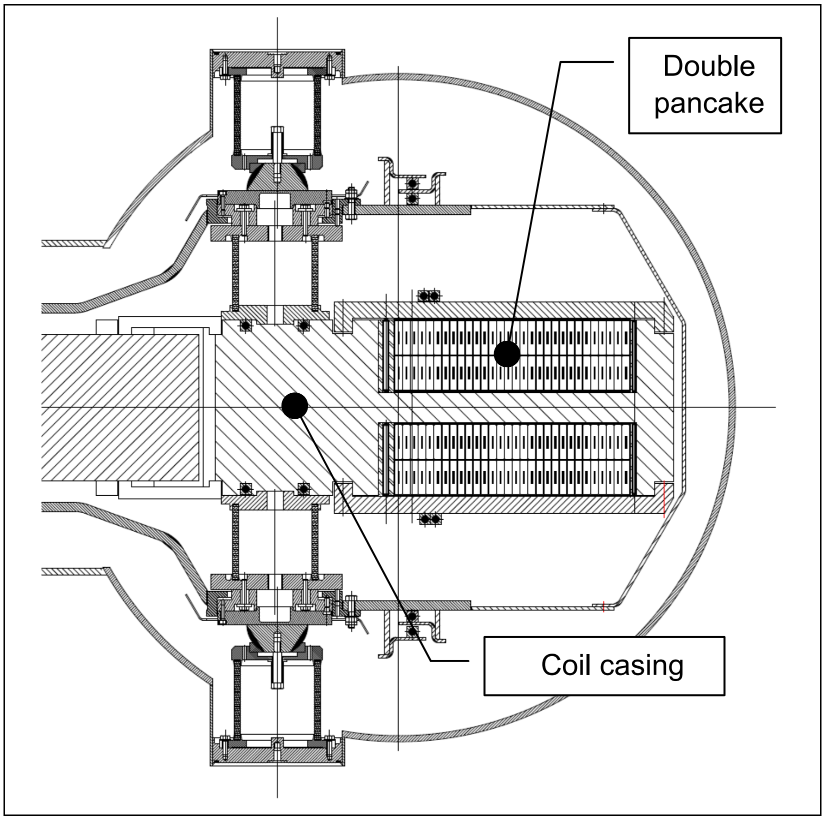

Figure 3.3: *Cross section BT coil.*

In figure 3.4 the order of the double pancakes are showed. One can see the position of the double pancakes in the coils, their connections and the names. The numbers from B1 till B8 are the 8 coils. Each coils has a face A and a face B. The double pancake at face A always consists of the pancakes 3 and 4. By this, face B is then always the pancakes 1 and 2.

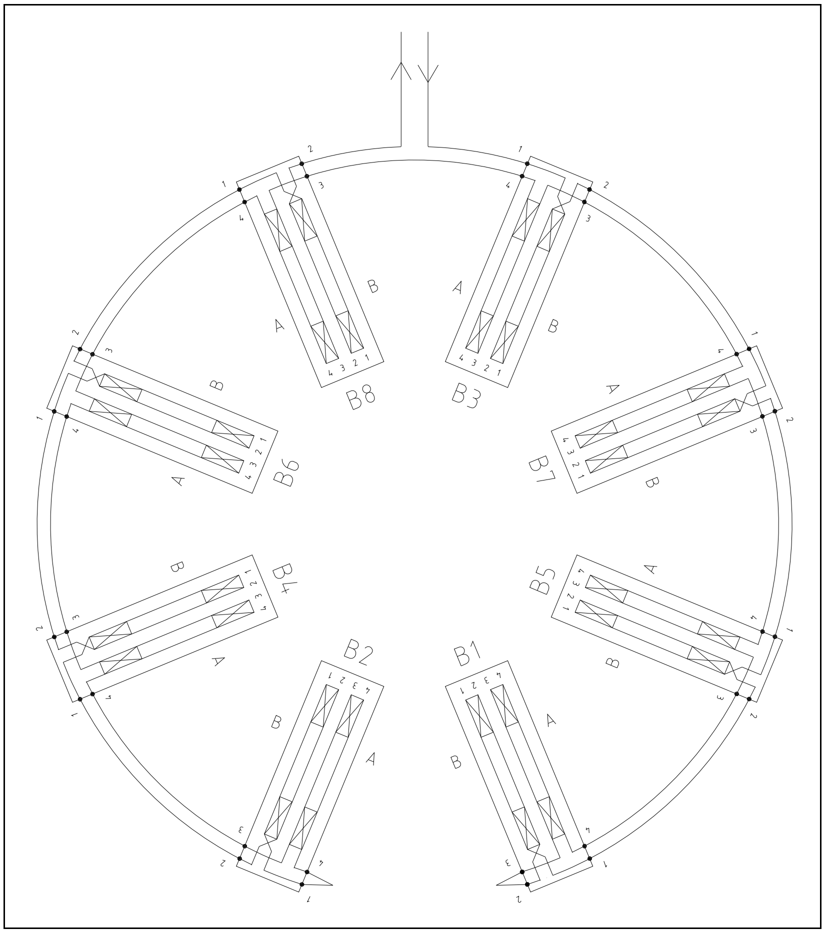

Figure 3.4: *Positions of double pancakes in BT.*

A pancake has 30 turns of superconducting cable. In the middle of this cable there are 32 strands with a diameter of 1.30 mm, made of Niobiumtitanium (NbTi) and copper (Cu). These strands are surrounded by pure aluminium (Al). A cross section of a cable can be seen in figure 3.5. The dimensions of the area of the conductor are 57 x 12 mm.

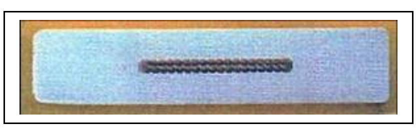

Figure 3.5: *Cross section cable.*

3.2 Control system

The control system is designed to check if all the processes of the magnet system are going correctly. The system is made so, that when something goes wrong, the power supply will be stopped and all the energy will be withdrawn from the system into external resistors. This process is called the slow dump. The time for the slow dump is about 130 minutes.

Depending on the emergency, a slow dump or a fast dump can be started. Basically the fast dump is the same as the slow dump, but in addition heaters on the superconducting cables are used to dissipate the energy of the magnet internally. The heaters make the temperature rise, then the cables are not superconducting anymore and they get a resistance. Because of the resistance, energy is dissipated in the coils and so the temperatures and the resistance will increase further. For a fast dump, the duration of the dump takes only 80 seconds.

The fast dump causes an interruption of the entire experiment, because the coils warmed up during the dump. It will take a few days to recool the coils again.

To control if everything is all right, voltage bridges are used. In the figure 3.6 a till c the bridges are illustrated. The bridges are calculated as follows:

Figure 3.6a → named 2-2:

    Voltage at plus pole minus voltage at minus pole

Figure 3.6b → named 1-3 +:

    Voltage at plus pole minus voltage at minus pole

Figure 3.6c → named 1-3 -:

    Voltage at minus pole minus voltage at plus pole

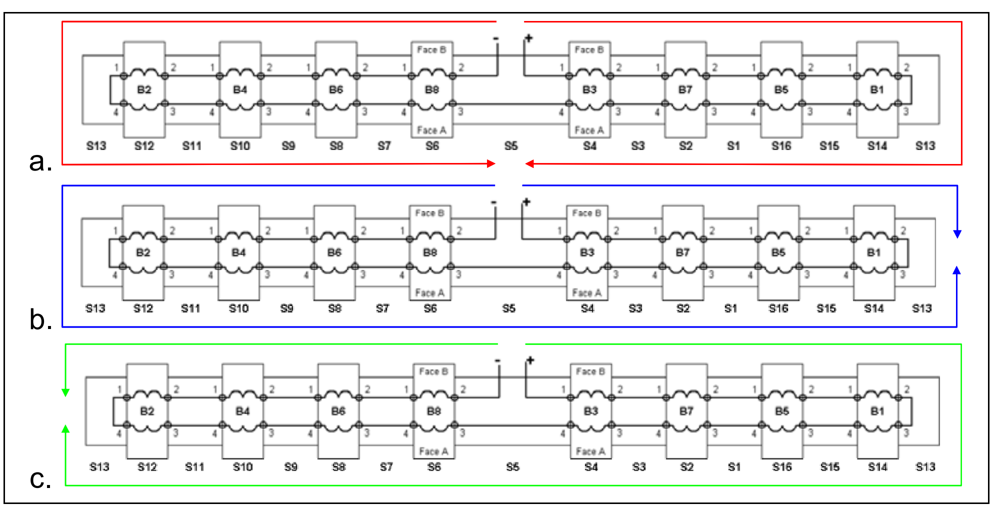

Figure 3.6: *Calculation of bridges.*

In the real control system the bridge voltages shown in the figure above are measured. For the calculations and simulations, the voltages of the bridges are calculated with the double pancake voltages.

The Barrel Toroid has been tested separately. At slow dump the control system gave an alarm that the value of one bridge was too high. So the difference between the voltages over the conductors was too high and the fast dump had to be started. The alarm was not correct, because of some sort of phenomenon observed in the first few seconds after start of the discharge. In the following graph the start of a slow dump is shown. One can see that the voltages over the pancakes are more different in the beginning then after roughly 5 seconds.

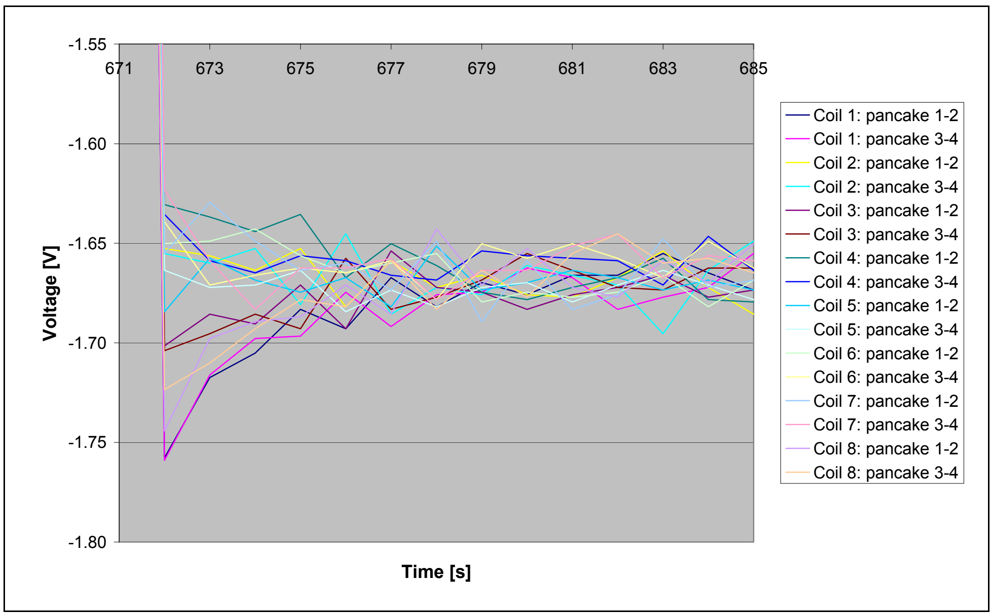

Figure 3.7: *Voltages over the double pancakes at start of slow dump.*

One of possible explanation of this effect is that the changing current through the conductor may induce currents in the coil casing around. These currents are not necessary similar to each other. With the simulations in the report an explanation is tried to be found for the start phenomenon of the slow dump of the ATLAS detector.

3.3 Electrical circuit

In the figure underneath a simple circuit is drawn. It represents a superconducting magnet (which means that it has no resistance) in serie with a resistance and a diode.

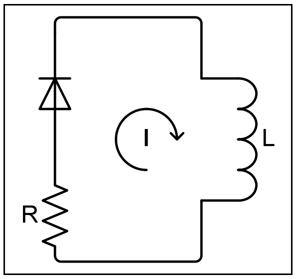

Figure 3.8: *Example circuit.*

Let the current have a start value, this means that the coil contains some stored magnetic energy. Because of the current that goes through the resistance, energy dissipates. This energy is withdrawn from the system and so the current decays and the energy of the inductor decreases.

When there is a current in the circuit in the direction shown in the figure, then the voltage over the diode is around 0.7 V. But in the case that there would be no current or a current in the opposite direction (which would be stopped by the diode), then the voltage over the diodes can have every value lower then 0.7 V. If there is a voltage over the diode, energy will be dissipated in the diode. When more energy is dissipated, then the current decay and the discharge will happen faster.

The energy of the BT is dissipated in 131 minutes during the slow dump with the use of a dump resistor of 0.001 Ω and 7 diodes. With a higher resistance, this time could be shortened. But in that case, high voltages (1 Ω means a voltage of 20.5 kV) will stand over the resistance. This would be an extra danger, which needs extra safety rules. That is why there is chosen for a resistance of 0.001 Ω. The maximum voltage will be around 20 V, which dissipates roughly 420.000 J/s in the beginning of the dump.

In figure 3.9, the electrical scheme of the Barrel Toroid and the End-Cap Toroids is shown. (The Central Solenoid has an own electrical circuit and that is why it is not described in the assignment.) In appendix A.2[(3)] the electrical properties of the BT are listed.

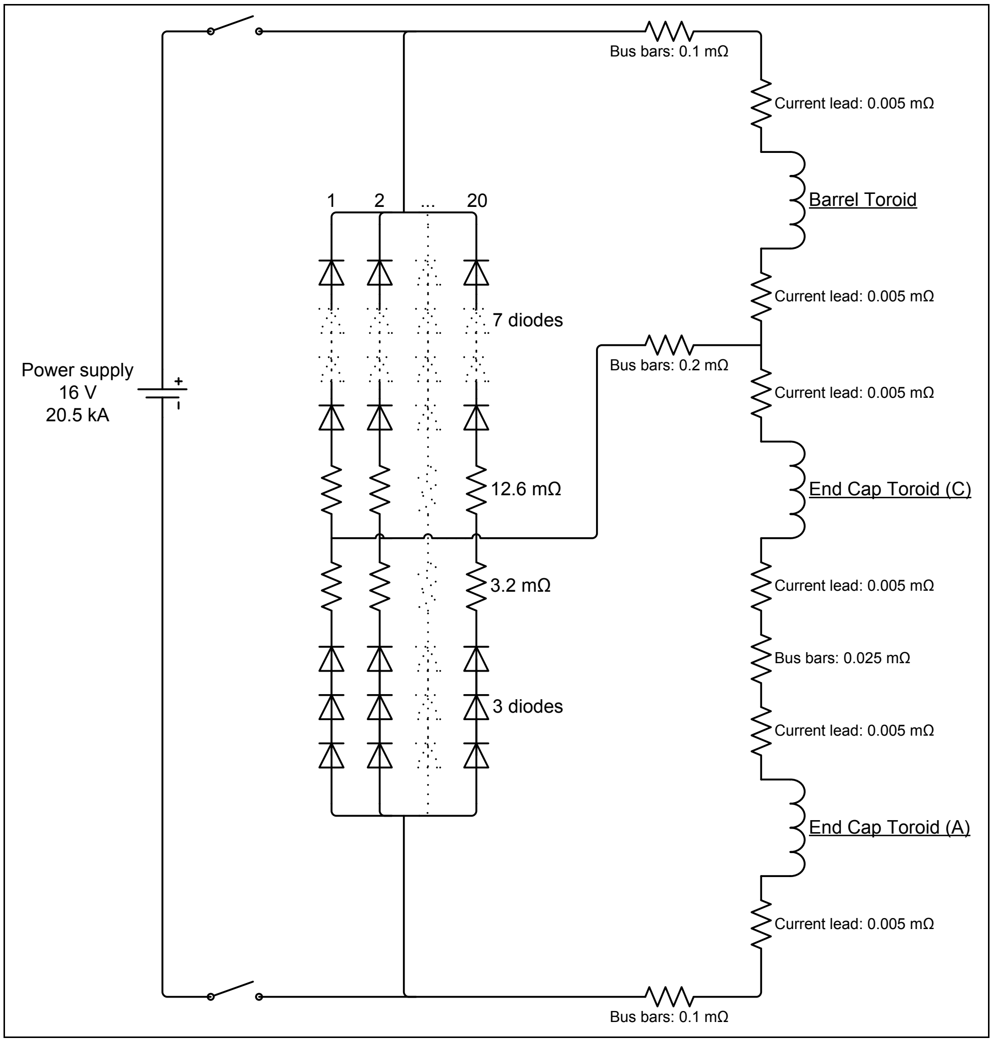

Figure 3.9: *Electrical circuit BT and ECTs.*

The main function of the diodes is that they lead the current through the coils, when the power supply is on (switches closed). When the diodes would not be there, a current would also go through the dump resistors, which would be useless. The diodes are also used to dissipate energy from the system and they provide a faster discharge when the current is at low values.

During the BT tests, the scheme is like shown in figure 3.10. The measurements are done in this configuration and this scheme is simulated. The construction of the bus bars was not that far completed, so cables were used instead of bus bars. These cables have a higher resistance, of which the value is measured. It appeared that the resistance was 0.33 mΩ.

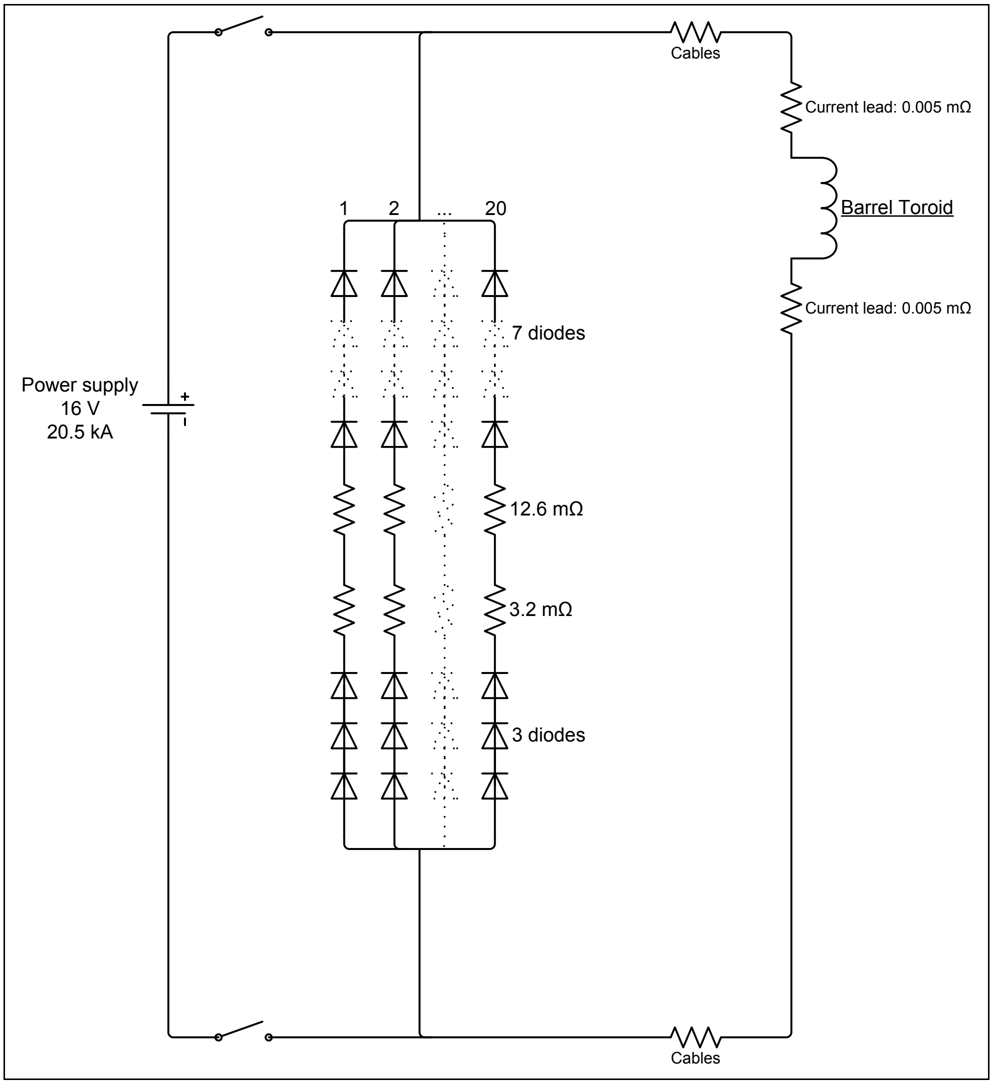

Figure 3.10: *Electrical circuit during BT tests.*

For the simulation of the discharge, the electrical scheme during the BT test can be simplified. Because the switches are open during the dump, the power supply does not have to be shown in a simplified circuit. There are 20 branches in the dump unit with each 10 diodes and 2 resistances. This is to split the current. Through one branch, not 20.5 kA, but roughly 1 kA of current will flow.

For the simulation, the number of diodes is not important. So the 10 diodes can be represented by one diode with a voltage of $10 \cdot 0.7 = 7\,\text{V}$. Assuming that the diodes do not have a resistance, an equivalent resistance can be calculated for the whole circuit by:

$$\frac{1}{20\left(\frac{1}{12.6}+\frac{1}{3.2}\right)}+0.01+0.33=1.13\,\text{m}\Omega$$

By this, the BT test circuit can be simplified as:

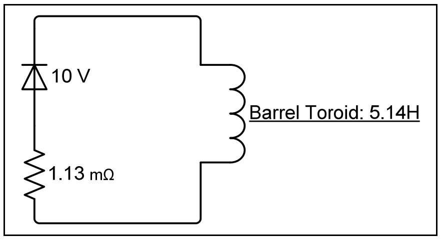

Figure 3.11: *Simplified electrical circuit during BT tests.*

This scheme is used in the coming simulations.

3.4 Simulation

In the simulation of the electrical circuit a numerical method is chosen. In the numerical method a new value will be calculated with the previous value, according to the following principle:

$$X_{i+1} = X_i + \left.\frac{dX}{dt}\right|_i \Delta t \qquad (1)$$

The variable Δt is the time between two calculate points. When i is multiplied by Δt, the result is the actual time. The change of X is at the moment i. This change is the unknown in the formula and will be derived in every step. In the two simulations in the next two chapters, the system will be defined in this change.

4 Simulation of one coil

In this chapter, the first simulation made, is explained and evaluated. The simulation is used to get knowledge of the system. In the first paragraph is explained which formulas are used and derived. The input values and results are shown in the second paragraph. In the last paragraph a conclusion is given about the simulation.

4.1 Theory

4.1.1 Definitions

The scheme that will be simulated is one coil with a secondary coil as shown in the figure 4.1. The primary coil represents the whole Barrel Toroid and the secondary circuit simulates the casing of the BT. Note that in the BT there are eight separate casings, one per coil. In this simulation the eight casings will be simulated as one.

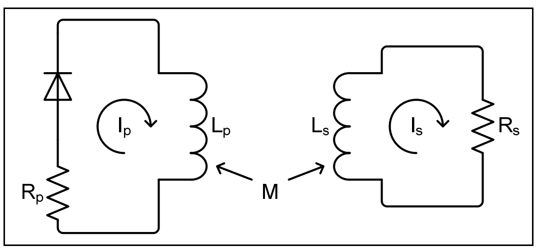

Figure 4.1: *Scheme of simulation 1.*

The following table describes the symbols which are used:

Table 4.2: *Symbols used in simulation 1.*

Name and unit	Primary coil	Secondary coil
Voltage [V]	Total: U_p Resistance: U_{Rp} Inductor: U_{Lp} Diode: U_d	Total: U_s Resistance: U_{Rs} Inductor: U_{Ls}
Current [A]	I_p	I_s
Resistance [Ω]	R_p	R_s
Inductance [H]	L_p	L_s
Mutual inductance [H]	M	

The voltages and the currents are variables with respect to the time. This will not always be shown in the symbols in this report, but should not be forgotten.

4.1.2 Formulas

With the use of formula 1, the formulas 2a and 2b can be defined for the currents in the primary and secondary circuits:

$$I_{p_{i+1}} = I_{p_i} + \left.\frac{dI_p}{dt}\right|_i \Delta t \tag{2a}$$

$$I_{s_{i+1}} = I_{s_i} + \left.\frac{dI_s}{dt}\right|_i \Delta t \tag{2b}$$

In these formulas the changes of the current are unknown. Expressions for these changes can be derived from the equations of the voltages in the circuits:

$$U_p = U_{Rp} + U_{Lp} + U_d = 0 \tag{3a}$$

$$U_s = U_{Rs} + U_{Ls} = 0 \tag{3b}$$

Because there is no voltage source in the circuits, the total voltages U_p and U_s are zero.

The voltage over the primary inductor is given by the formula:

$$U_{Lp} = L_p \frac{dI_p}{dt} + M \frac{dI_s}{dt} \tag{4}$$

Analogically, the voltage over the secondary coil can be defined, with the following final equations for the overall voltages as result:

$$U_p = R_p I_p + L_p \frac{dI_p}{dt} + M \frac{dI_s}{dt} + U_d = 0$$

$$U_s = R_s I_s + L_s \frac{dI_s}{dt} + M \frac{dI_p}{dt} = 0$$

In the following calculations there will be assumed that U_d is constant, so that the two changes can be calculated. The change for the secondary current will be derived from the formula of the secondary voltage:

$$\frac{dI_s}{dt} = -\frac{R_s}{L_s} I_s - \frac{M}{L_s} \frac{dI_p}{dt}$$

This change will be used in the formula for the primary voltage:

$$R_p I_p + L_p \frac{dI_p}{dt} - \frac{M R_s}{L_s} I_s - \frac{M^2}{L_s} \frac{dI_p}{dt} + U_d = 0$$

Now a result for the change in the primary current can be derived:

$$\frac{dI_p}{dt} = \frac{-R_p I_p + \frac{M R_s}{L_s} I_s - U_d}{L_p - \frac{M^2}{L_s}} = \frac{-L_s R_p I_p + M R_s I_s - L_s U_d}{L_p L_s - M^2} \tag{5a}$$

With total voltage U_s and the just derived $\frac{dI_p}{dt}$, one can calculate the change in the secondary current:

$$R_s I_s + L_s \frac{dI_s}{dt} + M \frac{-L_s R_p I_p + M R_s I_s - L_s U_d}{L_p L_s - M^2} = 0$$

The result for the change is:

$$\frac{dI_s}{dt} = -\frac{R_s}{L_s} I_s + \frac{M}{L_s} \frac{L_s R_p I_p - M R_s I_s + L_s U_d}{L_p L_s - M^2}$$

This can also be written as:

$$\frac{dI_s}{dt} = -\frac{R_s}{L_s} I_s + \frac{M R_p}{L_p L_s - M^2} I_p - \frac{M^2 R_s}{L_s \left(L_p L_s - M^2\right)} I_s + \frac{M}{L_p L_s - M^2} U_d$$

With the use of the following:

$$-\frac{1}{L_s} - \frac{M^2}{L_s\left(L_p L_s - M^2\right)} = \frac{-L_p L_s + M^2}{L_s\left(L_p L_s - M^2\right)} - \frac{M^2}{L_s\left(L_p L_s - M^2\right)} = \frac{-L_p}{L_p L_s - M^2}$$

The final formula for the change in the secondary current becomes:

$$\frac{dI_s}{dt} = \frac{M}{L_p L_s - M^2}\left(R_p I_p + U_d\right) - \frac{L_p R_s}{L_p L_s - M^2} I_s \qquad \text{(5b)}$$

There was assumed that the voltage over the diode was known, but that is not always true. In the beginning $I_p > 0$, so the voltage over the diode will be around 0.7V. When I_p would be zero or less, then I_p will be zero, because of the diode in the circuit. In this situation, the equations 3a and 3b become:

$$M \frac{dI_s}{dt} + U_d = 0$$

$$R_s I_s + L_s \frac{dI_s}{dt} = 0$$

The change in the primary current is zero. When there is no current in case calculated above, then there will also not be a change in the current. With the two formulas, U_d can be derived:

$$R_s I_s + L_s \frac{dI_s}{dt} = 0 \rightarrow \frac{dI_s}{dt} = -\frac{R_s I_s}{L_s}$$

$$M \frac{dI_s}{dt} + U_d = 0 \rightarrow -M \frac{R_s I_s}{L_s} + U_d = 0 \rightarrow U_d = \frac{M R_s I_s}{L_s} \qquad \text{(6)}$$

The part of the simulation with the formulas is showed in figure 4.3 (the total simulation can be found in appendix B). As showed in the formulas 3a and b, i will be the counter in the simulation.

$$\begin{pmatrix} U_{d_{i+1}} \\ I_{p_{i+1}} \\ I_{s_{i+1}} \end{pmatrix} := \begin{bmatrix} \text{if}\left[\left(I_{p_i} + \dfrac{-R_p \cdot I_{p_i} + \dfrac{M \cdot R_s}{L_s} \cdot I_{s_i} - U_{d_0}}{L_p - \dfrac{M^2}{L_s}} \cdot \Delta t\right) \le 0, \dfrac{M \cdot R_s}{L_s} \cdot I_{s_i}, U_{d_0}\right] \\ \text{if}\left[\left(I_{p_i} + \dfrac{-R_p \cdot I_{p_i} + \dfrac{M \cdot R_s}{L_s} \cdot I_{s_i} - U_{d_i}}{L_p - \dfrac{M^2}{L_s}} \cdot \Delta t\right) \le 0, 0, \left(I_{p_i} + \dfrac{-R_p \cdot I_{p_i} + \dfrac{M \cdot R_s}{L_s} \cdot I_{s_i} - U_{d_i}}{L_p - \dfrac{M^2}{L_s}} \cdot \Delta t\right)\right] \\ I_{s_i} + \left[\dfrac{M}{L_p \cdot L_s - M^2} \cdot \left(R_p \cdot I_{p_i} + U_{d_i}\right) - \dfrac{L_p \cdot R_s}{L_p \cdot L_s - M^2} \cdot I_{s_i}\right] \cdot \Delta t \end{bmatrix}$$

Figure 4.3: *Part with formulas of simulation 1.*

In the simulation U_{d0} is defined as the voltage over the diode in the case of a primary current above zero. The primary current is calculated, but when the result is smaller or equal to zero, then the current has to be set to zero. The formula for the voltage over the diode, is made by a comparison. When the current $I_p \le 0$, then the voltage over the diode is given by formula 6.

4.2 Results

All variables that had to be filled in the simulation are known, except the primary resistance and the voltage over the diode. Those had to be estimated. The chosen value for the diode voltage is also consistent with its specifications. All the values that were used to simulate the discharge of 20.5 kA are shown below:

Coil properties $R_p = 0.001145$ $R_s = \dfrac{14 \cdot 10^{-6}}{8}$

$L_p = 5.1416$ $L_s = \dfrac{52 \cdot 10^{-6}}{8}$

$M = \dfrac{5.5 \cdot 10^{-3}}{8}$

Initial values $I_p = 20479$ $I_s = 0$

$U_d = 10 \cdot 0.665$

The electrical properties of the coil casing are divided by 8, because the eight coil casings can be seen as eight parallel circuits.

After fitting of several measurements, the value for the diode voltage presented above, was found. By fitting is meant that the data and the simulation had to have the same discharge time and the curves also had to have the same shape. Each measurement had a different value for the primary resistance. A possible explanation follows a little bit further in this paragraph. Note that the primary resistance represents the resistance of the total circuit, so besides the dump resistors, also the resistances of the bus bars and the cables. This value was estimated as 1.13 mΩ, which is almost the same.

In figure 4.4 one can see the plots of the primary and secondary current. The x-axis is the actual time, i multiplied by Δt.

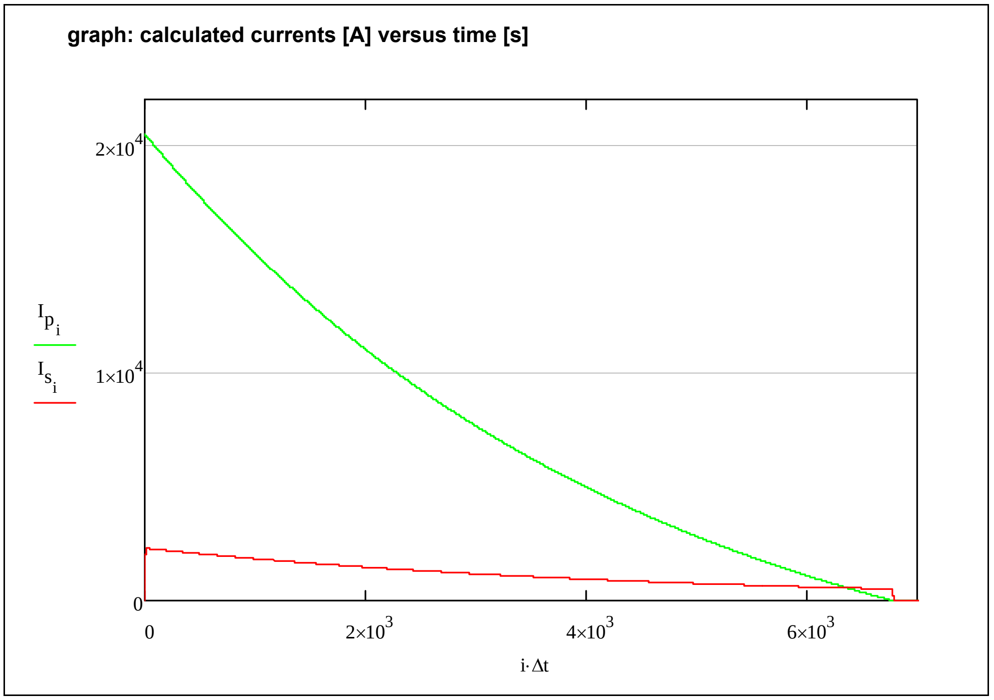

Figure 4.4: *Graph with calculated currents of simulation 1.*

According to the graph, one could think that there is a significant secondary current. The top of the graph is almost 2300 A. But with some calculations it appears that this is not the case. The theoretical energy that was in the system at the start can be calculated as follows:

$$E_{th} = \frac{1}{2} L_p I_p{}^2 = \frac{1}{2} 5.1416 \cdot 20479^2 = 1.078 \cdot 10^9 \text{ J} \qquad (7)$$

When the maximum energy in the coil of the secondary circuit is calculated, then the following value is the result:

$$E_{th} = \frac{1}{2} L_s I_s^{\ 2} = \frac{1}{2} \frac{52 \cdot 10^{-6}}{8} \cdot 2300^2 = 17 \text{ J}$$

This shows that the energy in the casing (note that this is an equivalent casing to eight reel casings) is almost nothing with respect to the superconducting coils. Another way to show this is by the voltage over the resistance:

Primary resistance: $0.00145 \cdot 20500 = 23.5 \text{ V}$

Secondary resistance: $\frac{14 \cdot 10^{-6}}{8} 2300 = 0.004 \text{ V}$

Concluding, the secondary current is in these aspects not so important, because the properties of the circuits differ very much.

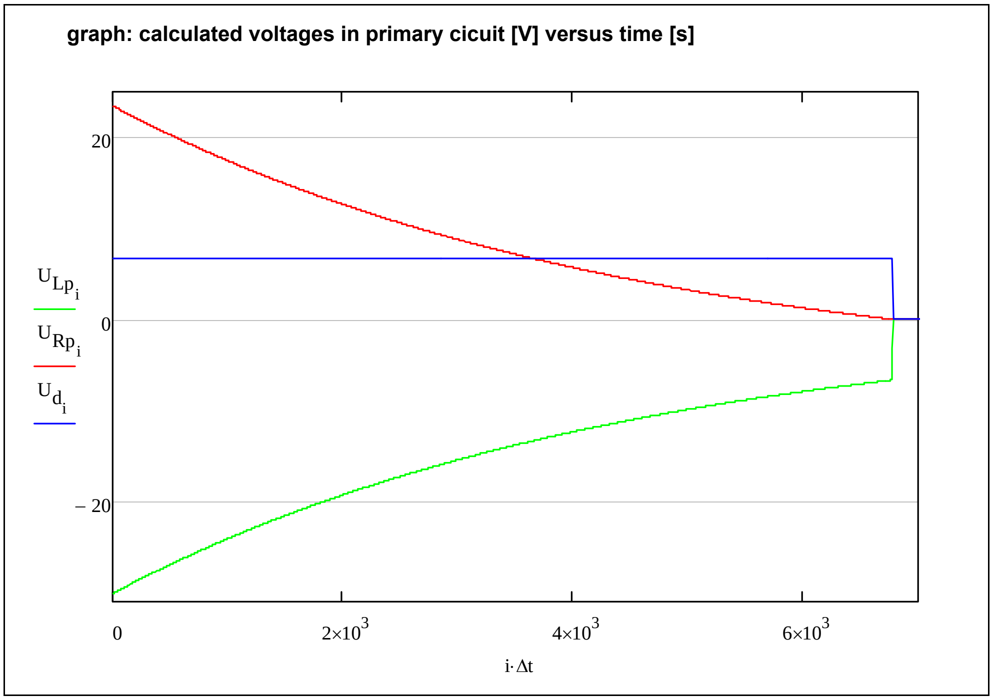

Figure 4.5: *Graph with calculated voltages of simulation 1.*

Figure 4.5 shows that the voltage over the diode is constant at 10 times 0.665V, until the point where there is no current anymore. Because of the zero current, the resistance is also zero. At $i\Delta t = t = 0$ the current starts to decay and so the term of the change in the primary current in formula 4 is negative. This explains the negative voltage over the primary coil. As specified in formula 4a, the voltage over the resistance and the diode is the opposite of the voltage over the inductor.

A way to see if the simulation is correct is to look at the energy dissipation. It is already calculated that the theoretical energy in the system at the beginning of the slow dump is $1.078 \cdot 10^9$ J. The energy is also calculated with the integration of the power (power of primary and secondary resistance, plus the power of the diode) in the simulation (appendix B):

$$E = \sum_i P\Delta t = 1.078 \cdot 10^9 \text{ J} \quad (8)$$

These values are the same, what shows that the simulation is correct.

The calculation showed that 68% of the energy was dissipated in the primary resistance and 32% in de diode. In the coil casing only 0.002% of the total energy is generated due to the small resistance.

Off course, it is more important that the calculated currents and voltages are the same as the measured data. In the following two figures 4.6 and 4.7, graphs are shown of the calculated (black dashed) and measured (red straight) values of the current and voltage. The measurement is used in which the BT was discharged from 20.5 kA.

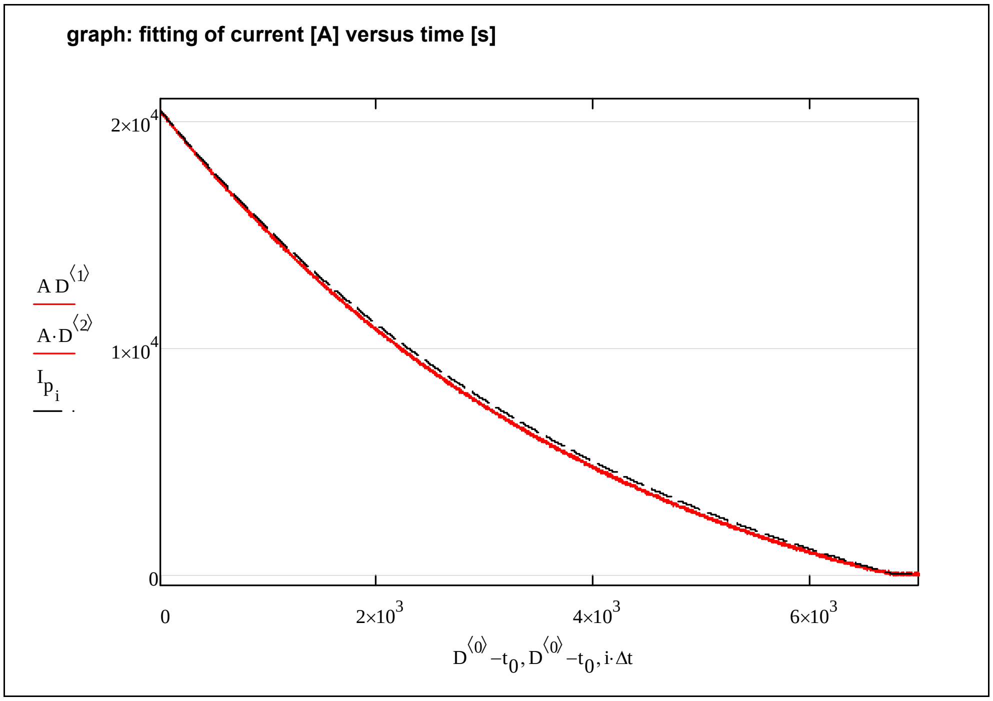

Figure 4.6: *Graph with fitted current of simulation 1.*

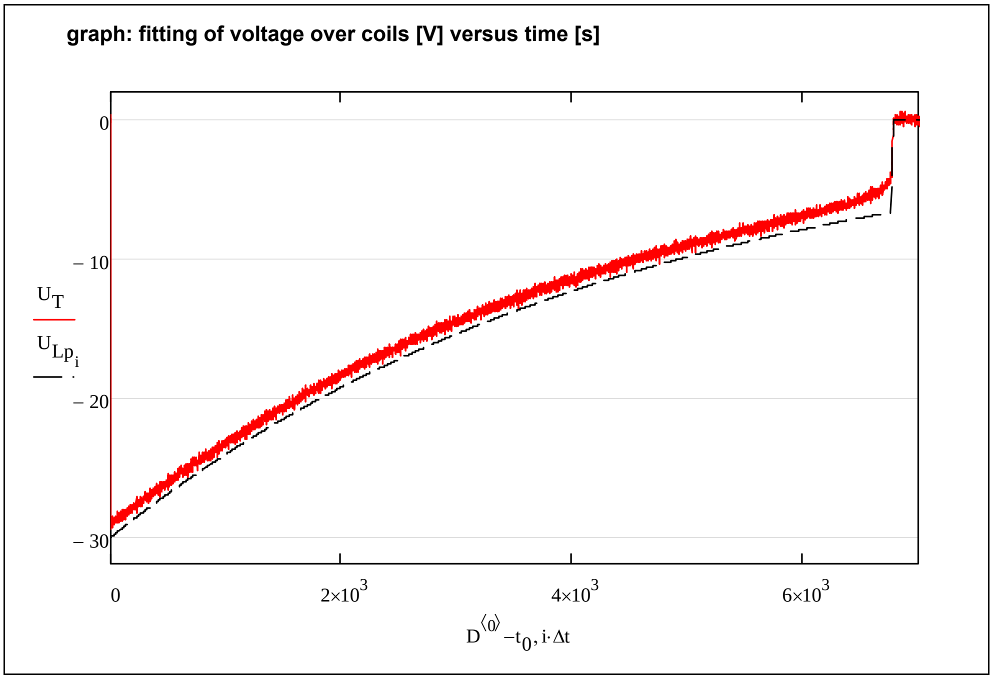

Figure 4.7: *Graph with fitted voltage of simulation 1.*

As one can see from the figures, the simulation of the measurement is pretty the same as the measured data. A little difference in the graphs can be seen. An explanation could be that the voltage over the diode is not constant during the whole measurement. It may be that it dependents on the temperature and the current going through the diode. Also the resistance of the bus bars and cables can change during the measurement as function of the temperature.

4.3 Conclusion

The simulation of the Barrel Toroid as one coil with an induced coil as the coil casings is made. The results of the simulation are as expected. The simulation is good and precise enough to reproduce the measurements. By the development of the simulation, the effect of each component in the total scheme is known. The simulation can now be extended for the simulation of the voltages over each of the eight coils.

5 Simulation of eight coils

The second simulation is to investigate if a variation in the resistances of the coil casings could be responsible for the strange phenomenon in the beginning of the slow dump. Now it is necessary to simulate the voltage over each coil of the Barrel Toroid. The outline is the as the previous one.

5.1 Theory

5.1.1 Definitions

The scheme that will be simulated is drawn in figure 5.1.

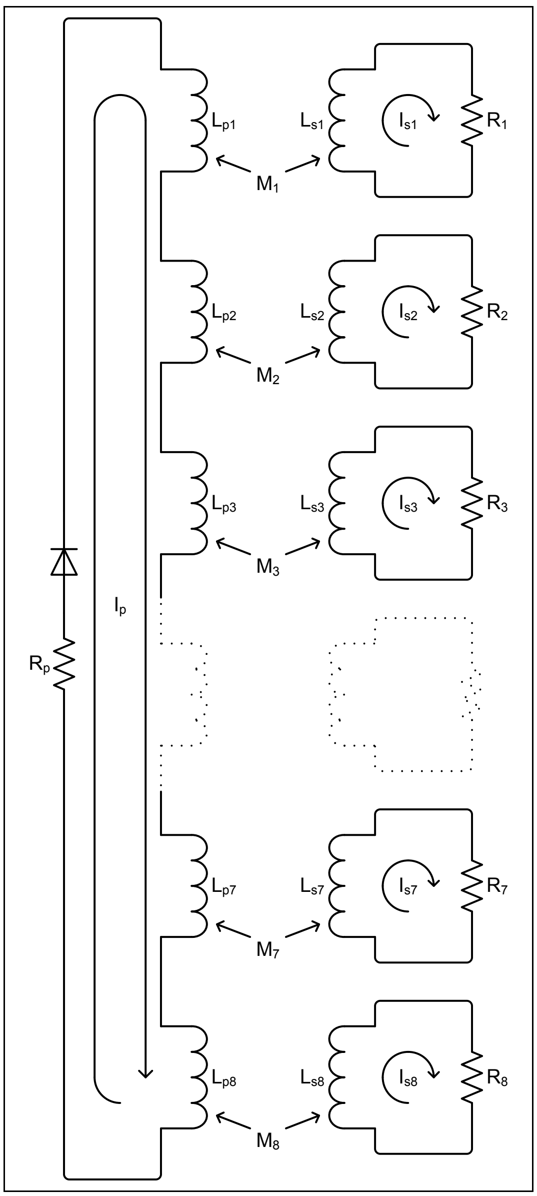

Figure 5.1: *Scheme of simulation 2.*

Only the voltage over the coil will be calculated in the simulation. There will be assumed that the voltages over two double pancakes in a coil are the same.

The following table describes the symbols which are used:

Table 5.2: *Symbols used in simulation 2.*

Name and unit	Primary coil	Secondary coil
Voltage [V]	Total: U_p Resistance: $U_{R\,p}$ Inductor: $U_{L\,p_n}$ Diode: U_d	Total: $U_{s\,n}$ Resistance: $U_{R\,n}$ Inductor: U_{Lsn}
Current [A]	I_p	$I_{s\,n}$
Resistance [Ω]	R_p	R_n
Inductance [H]	$L_{p\,n}$	$L_{s\,n}$
Mutual inductance [H]	M_n	

In the symbols n is the counter for the eight coils in the BT (like the counter i for time), so $n = 1,2..N$ with $N = 8$.

5.1.2 Formulas

The formulas for the current and voltages in the primary and secondary circuits are basically the same as the ones in the previous simulation. The only difference is that there are eight coils instead of one:

$$I_{p_{i+1}} = I_{p_i} + \left.\frac{dI_p}{dt}\right|_i \Delta t \tag{9a}$$

$$I_{s\,i+1,n} = I_{s\,i,n} + \left.\frac{dI_{s\,n}}{dt}\right|_i \Delta t \tag{9b}$$

$$U_p = R_p I_p + \frac{dI_p}{dt}\sum_n \left(L_{p_n}\right) + \sum_n \left(M_n \frac{dI_{sn}}{dt}\right) + U_d = 0 \tag{10a}$$

$$U_{s\,n} = R_n I_{s\,n} + L_{s\,n}\frac{dI_{s\,n}}{dt} + M_n \frac{dI_p}{dt} = 0 \tag{10b}$$

From the formula $U_{s\,n}$ the change in the secondary current can be derived:

$$\frac{dI_{sn}}{dt} = -\frac{R_n}{L_{sn}} I_{sn} - \frac{M_n}{L_{sn}} \frac{dI_p}{dt}$$

This will be used in the formula for the primary voltage to get the change of the primary current:

$$R_p I_p + \frac{dI_p}{dt} \sum_n \left(L_{p_n} \right) + \sum_n \left(-\frac{M_n R_n}{L_{sn}} I_{sn} - \frac{{M_n}^2}{L_{sn}} \frac{dI_p}{dt} \right) + U_d = 0$$

$$R_p I_p + \frac{dI_p}{dt} \sum_n \left(L_{p_n} \right) - \sum_n \left(\frac{M_n R_n}{L_{sn}} I_{sn} \right) - \frac{dI_p}{dt} \sum_n \left(\frac{{M_n}^2}{L_{sn}} \right) + U_d = 0$$

$$\frac{dI_p}{dt} = \frac{-R_p I_p + \sum_n \left(\frac{M_n R_n}{L_{sn}} I_{sn} \right) - U_d}{\sum_n \left(L_{p_n} \right) - \sum_n \left(\frac{{M_n}^2}{L_{sn}} \right)} \qquad (11a)$$

The result can be compared with the result of previous simulation. One can see that the formulas are almost the same, except some summations.

Formula 10b and 10a will be used to calculate $\frac{dI_{sn}}{dt}$:

$$R_n I_{sn} + L_{sn} \frac{dI_{sn}}{dt} + M_n \frac{-R_p I_p + \sum_n \left(\frac{M_n R_n}{L_{sn}} I_{sn} \right) - U_d}{\sum_n \left(L_{p_n} \right) - \sum_n \left(\frac{{M_n}^2}{L_{sn}} \right)} = 0$$

$$\frac{dI_{sn}}{dt} = -\frac{R_n}{L_{sn}} I_{sn} + \frac{M_n}{L_{sn}} \frac{R_p I_p - \sum_n \left(\frac{M_n R_n}{L_{sn}} I_{sn} \right) + U_d}{\sum_n \left(L_{p_n} \right) - \sum_n \left(\frac{{M_n}^2}{L_{sn}} \right)} \qquad (11b)$$

The formulas 11a and 11b can not be simplified because of the summations.

Again the voltage over the diodes has to be calculated. If $I_p \leq 0$ in this simulation, then the equations for the voltages (formulas 10a and 10b) become:

$$\sum_n \left(M_n \frac{dI_{sn}}{dt} \right) + U_d = 0$$

$$R_n I_{sn} + L_{sn} \frac{dI_{sn}}{dt} = 0$$

The result for U_d is:

$$R_n I_{s\,n} + L_{s\,n}\frac{dI_{s\,n}}{dt} = 0 \rightarrow \frac{dI_{s\,n}}{dt} = -\frac{R_n}{L_{s\,n}} I_{s\,n}$$

$$\sum_n \left(M_n \frac{dI_{s\,n}}{dt} \right) + U_d = 0 \rightarrow U_d = \sum_n \left(\frac{M_n R_n I_{s\,n}}{L_{s\,n}} \right) \qquad (12)$$

The part with the formulas integrated in Mathcad is shown underneath. The full simulation can be found in appendix C.

$$\begin{pmatrix} U_{d_{i+1}} \\ I_{p_{i+1}} \\ I_{s_{i+1,n}} \end{pmatrix} := \begin{bmatrix} \mathrm{if}\left[\left[I_{p_i} + \dfrac{-R_p \cdot I_{p_i} + \sum_n \left(\dfrac{M_n \cdot R_n}{L_{s_n}} \cdot I_{s_{i,n}} \right) - U_{d_0}}{\sum_n \left(L_{p_n} \right) - \sum_n \left[\dfrac{\left(M_n\right)^2}{L_{s_n}} \right]} \cdot \Delta t \right] \le 0, \sum_n \left(\dfrac{M_n \cdot R_n}{L_{s_n}} \cdot I_{s_{i,n}} \right), U_{d_0} \right] \\ \mathrm{if}\left[\left[I_{p_i} + \dfrac{-R_p \cdot I_{p_i} + \sum_n \left(\dfrac{M_n \cdot R_n}{L_{s_n}} \cdot I_{s_{i,n}} \right) - U_{d_i}}{\sum_n \left(L_{p_n} \right) - \sum_n \left[\dfrac{\left(M_n\right)^2}{L_{s_n}} \right]} \cdot \Delta t \right] \le 0, 0, \left[I_{p_i} + \dfrac{-R_p \cdot I_{p_i} + \sum_n \left(\dfrac{M_n \cdot R_n}{L_{s_n}} \cdot I_{s_{i,n}} \right) - U_{d_i}}{\sum_n \left(L_{p_n} \right) - \sum_n \left[\dfrac{\left(M_n\right)^2}{L_{s_n}} \right]} \cdot \Delta t \right] \right] \\ I_{s_{i,n}} + \left[-\dfrac{R_n}{L_{s_n}} \cdot I_{s_{i,n}} + \dfrac{M_n}{L_{s_n}} \cdot \dfrac{R_p \cdot I_{p_i} - \sum_n \left(\dfrac{M_n \cdot R_n}{L_{s_n}} \cdot I_{s_{i,n}} \right) + U_{d_i}}{\sum_n \left(L_{p_n} \right) - \sum_n \left[\dfrac{\left(M_n\right)^2}{L_{s_n}} \right]} \right] \cdot \Delta t \end{bmatrix}$$

Figure 5.3: *Part with formulas of simulation 2.*

5.2 Results

All variables that had to be filled in, were known, except the secondary resistances. All the values used to simulate the discharge of measurement 18 are shown below:

Coil properties	$R_p = 0.001172$	
	$L_{p_n} = 0.6427$	$L_{s\,n} = 52 \cdot 10^{-6}$
	$M_n = 5.5 \cdot 10^{-3}$	
Initial values	$I_p = 17976$	$I_{s\,n} = 0$
	$U_d = 10 \cdot 0.665$	

After fitting the simulation with the measurement, the values of the secondary resistance that were found, are listed in the table underneath.

Table 5.4: *Secondary resistances.*

Coil	R_s [10^{-6} Ω]	Δ [%]
1	14.52	3.6
2	13.79	-1.6
3	14.32	2.1
4	13.67	-2.5
5	13.94	-0.6
6	13.84	-1.3
7	13.8	-1.6
8	14.28	1.9

In the table there is used $\Delta = \frac{R_s - \overline{R_s}}{\overline{R_s}} 100\%$ with a mean value of $\overline{R_s} = 14.02 \cdot 10^{-6}\,\Omega$. The estimated value was $14 \cdot 10^{-6}\,\Omega$, so the fitting is done making variations in this value. In the following figure one can see a plot of the resistances in order of the configuration of the coils in the BT.

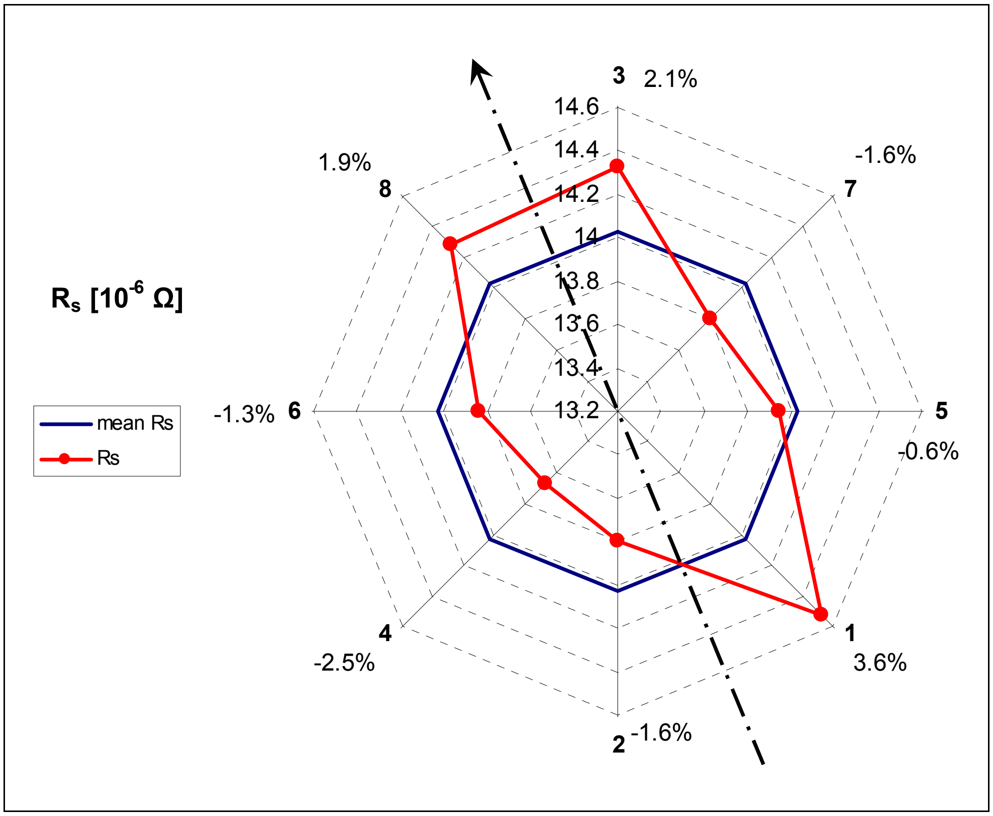

Figure 5.5: *Secondary resistances in the BT configuration (coil 3 and 8 on top).*

The results of the simulation are presented in the figure 5.6 (data is presented as red line, dashed black lines are simulated), figure 5.7 (data is presented as red line, dashed black line is simulated) and figure 5.8 (data is line, dashed lines are simulated).

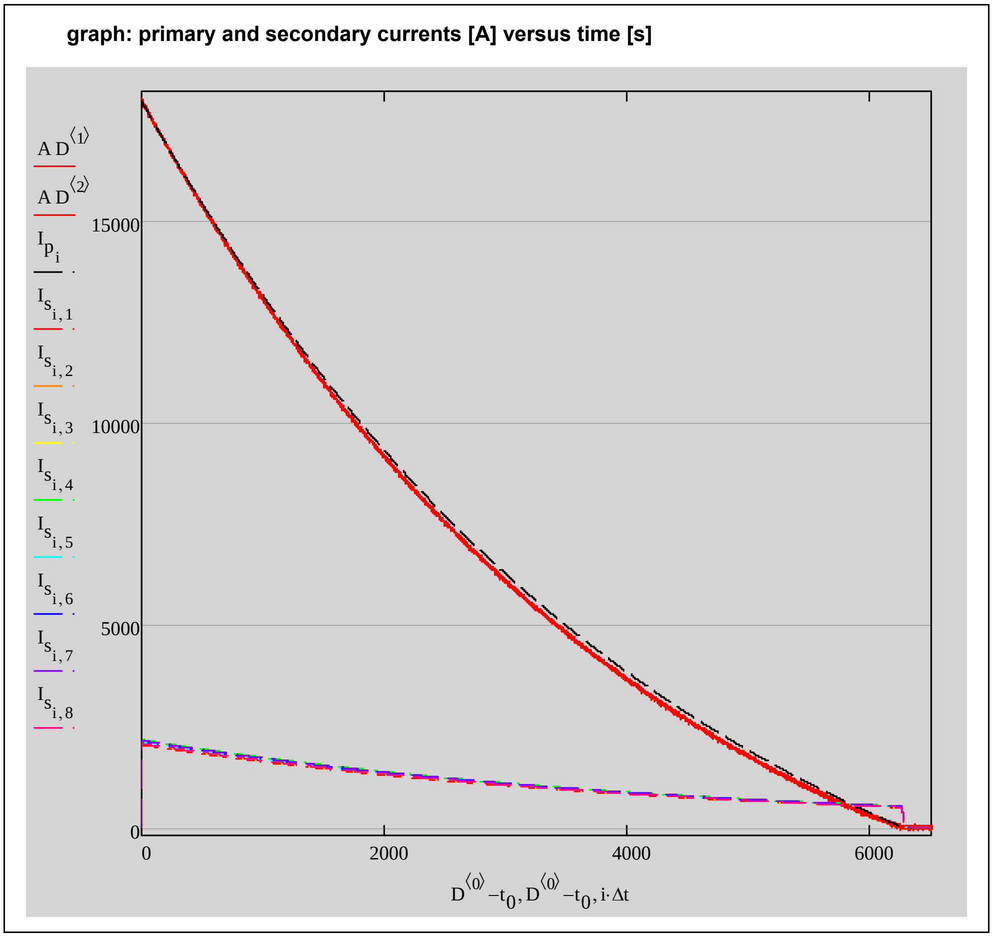

Figure 5.6: *Graph with currents of simulation 2.*

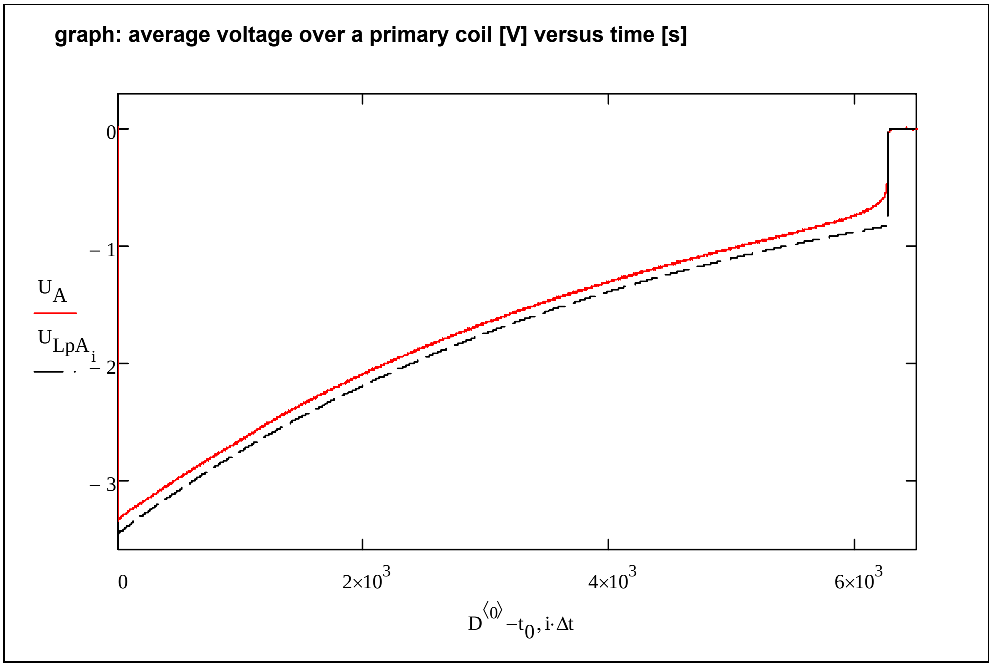

Figure 5.7: *Graph with voltages of simulation 2.*

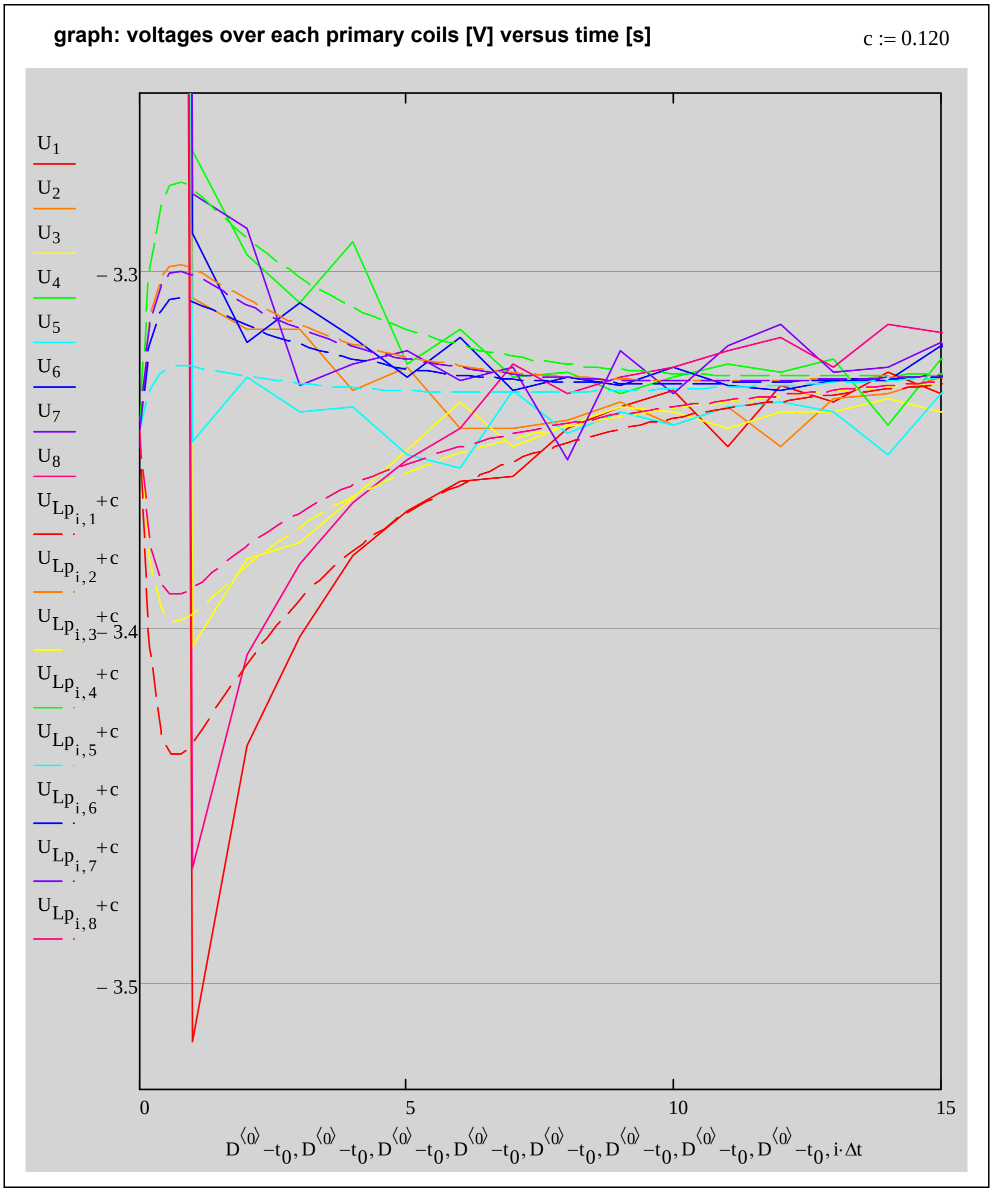

Figure 5.8: *Graph with double pancake voltages in the start of simulation 2.*

The complete simulation can be found in appendix C. Note: the coefficient c (figure 5.8) is used to lift the simulated graph a little bit for a better comparison of the eight coil voltages. This is because (as one can see in figure 5.7) the graphs are a little bit different.

The estimation of the secondary resistances (and so the coil voltages) was difficult and not exact. The simulation does not follow the data precisely, but it follows the trend, which is good enough. This is shown in figure 5.9, because the calculated bridges follow the measured bridges and exceed the threshold of 50 mV, just as the bridge of the measured data.

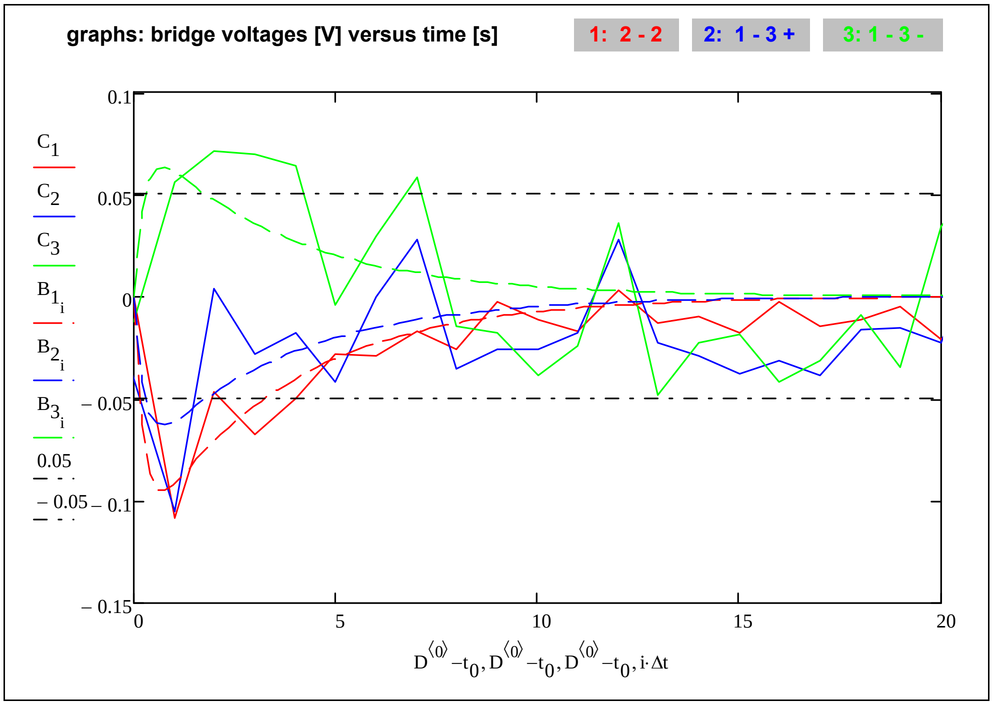

Figure 5.9: *Graph with bridge voltages in the start of simulation 2.*

5.3 Conclusion

The second simulation of the eight coils of the Barrel Toroid separately may describe the voltage difference. The goal to simulate the bridge voltages is reached. The simulation showed that with a maximum variation of 3.6%, around an average of $14.02 \cdot 10^{-6}\,\Omega$ in the casing resistance, can cause the phenomenon in the beginning of the slow dump.

6 Energy distribution

During the fast dump of a magnet, the stored energy is dissipated internally. By this dissipation, the temperature and the enthalpy of the material is rising. In this chapter calculations are done to estimate the amount of energy that is stored in the different parts of the magnet.

6.1 Method

During the fast dump, a part of the total energy dissipates in the dump unit. At the start of the dump, heaters make the temperature of the conductor rise. Because of this temperature rise, the coils are not superconducting anymore and so they get a resistance. The current and the resistance generate energy in the coils. This energy makes the temperature and enthalpy of the conductor rise. The dissipated energy also increases the temperature and the enthalpy of the insulation (fibreglass-epoxy G-10) and the coil casing.

With all these aspects, two equations for the energy can be defined:

$$E_{tot} = E_{cable} + E_{dump} \tag{13a}$$

$$E_{cable} = H_{cable} + E_{undefined} = H_{Al} + H_{Cu} + H_{insulation} + H_{casing} + E_{undefined} \tag{13b}$$

The total energy in the system (E_{tot}) is dissipating in the cable (E_{cable}) and in the dump unit (E_{dump}). The energy that goes into the cable will change the enthalpy of the cable (H_{cable}). E_{cable} and H_{cable} will be calculated and so there is an undefined part ($E_{undefined}$). All terms will be explained further on in this paragraph.

The enthalpy change of the cable can be calculated as the sum of the enthalpy changes of the aluminium part (H_{Al}), the copper (H_{Cu}), the insulation ($H_{insulation}$) and the casing (H_{casing}). (For the NbTi part of the cable, it is assumed that it has the same properties as copper.)

A material has at a certain temperature an enthalpy and a resistivity. With the resistivity and the properties of the wire, the resistance can be calculated:

$$R = \frac{l \cdot \rho}{A} \tag{14}$$

In this formula, R is the resistance [Ω] of a conductor, l is the length [m] and A is the area [m^2] of the cross section of the wire. The symbol ρ stands for the electrical resistivity [Ωm] of the conductor. In the rest of this report electrical resistivity is meant when there is said resistivity.

To calculate the enthalpy change of the different parts in formula 13b, the change in the temperature must be known. This temperature difference can be calculated with the change of the resistance.

From the fast dump measurements, the voltages and the current of all the double pancakes are known. With this data the change in the resistance can be estimated. Formula 15 shows that the voltage over a conductor consists of a resistive part, an inductive part and an induced inductive part.

$$U = IR + L\frac{dI_p}{dt} + M\frac{dI_s}{dt} \quad (15)$$

In the calculations the induced voltage is ignored, because this effect is not so big. So from formula 15 we can derive a new formula for the resistance of a double pancake, during a fast dump:

$$R = \frac{U - L\frac{dI_p}{dt}}{I} \quad (16)$$

For a measurement, the result will be a graph of the resistance versus time. The resistance is zero at the beginning of the fast dump, but later it has a certain value. With the maximum resistance, the maximum resistivity and the maximum temperature can be calculated. With the highest temperature, the highest enthalpy of the material is also known. On this way the stored energy in the different parts can be calculated.

It is assumed that the temperatures of the cable (the aluminium part and the superconducting part) and the insulation are the same. The stored energy in these parts can be calculated by using the temperature and the different material properties.

For the enthalpy change of the coil casing, the temperature sensors of the pancakes are used. These sensors are located on the surface of the coil casing, so they measure the temperature of the casing and not of the coils themselves. Like that, this value for the temperature can be used to calculate the amount of energy in the coil casing (same as method for the cable).

The energy that goes into the dump unit can be calculated with the total voltage over all the coils:

$$E_{dump} = \int I(U_1 + U_2 + ... + U_8)dt = \Delta t \sum_{i=0}^{t_{max}} I(U_1 + U_2 + ... + U_8)$$

This energy must be calculated until time t_{max} at which the resistance (and temperature) of the conductor is the highest. During the calculations, t_{max} is estimated for every double pancake.

To calculate the total dissipated energy in the conductor, the product of the current and the resistive voltage of the double pancake must be integrated:

$$E_{int} = \int IU_R dt = \Delta t \sum_{i=0}^{t_{max}} IU_R$$

How all the calculations explained above are done, will be shown with the use of real data in the next paragraph.

6.2 Calculations

For the measurements done during a fast dump from 20.5 kA of the BT, the energy dissipation is calculated. All terms of the following equations have to be calculated:

$$E_{tot} = E_{cable} + E_{dump} \tag{13a}$$

$$E_{cable} = H_{cable} + E_{undefined} = H_{Al} + H_{Cu} + H_{insulation} + H_{casing} + E_{undefined} \tag{13b}$$

All calculations are done for every double pancake. Only for double pancake A in coil 3, the calculations will be shown and explained in this paragraph as an example.

In the graph of figure 6.1 the measured voltages of the 16 double pancakes of BT are presented during a fast dump from 20.5 kA.

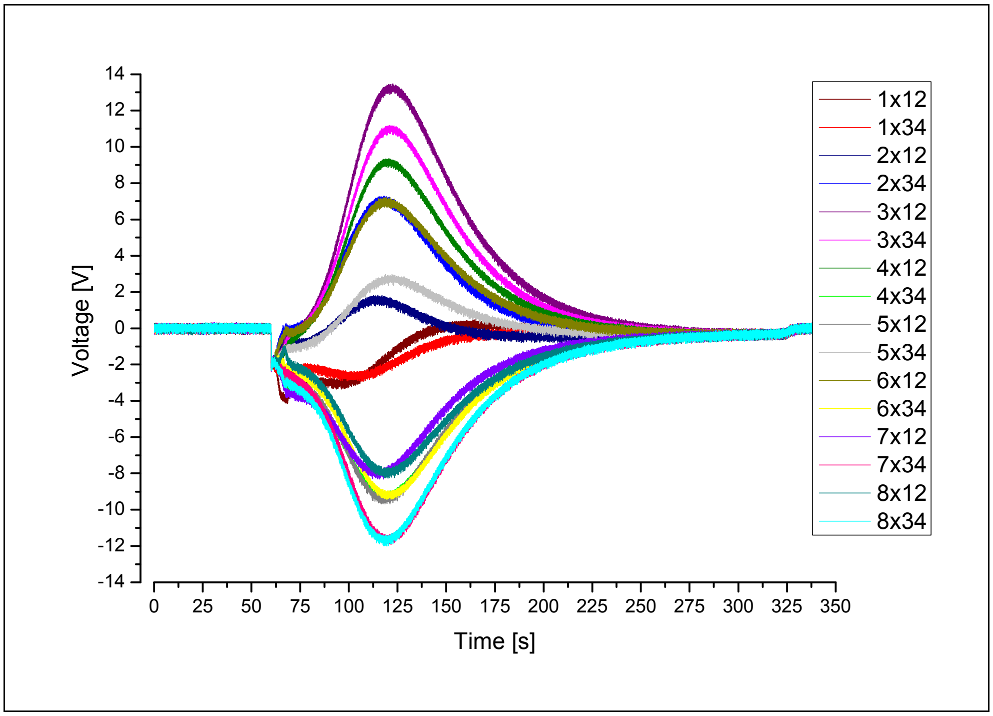

Figure 6.1: *Measured voltages of double pancakes during fast dump.*

In the graph of the voltages of the double pancakes, one can see that the fast dump starts around 60 s. Then in 8 seconds, all the conductors leave the superconducting state. The voltages keep increasing (positively and negatively) until the current is too low. The voltages are at their top (maximum or minimum) and then they descent with the current. The voltages are nicely spread positively and negatively. This is due to different resistances (temperatures) of the double pancakes. When all voltages are summed, then the result is the typical discharge curve during a dump. The two double pancakes of coil 1 behave a little bit different, because one heater has a longer reaction time. That's why the resistance (and so the voltage) is not so high.

In figure 6.2 the graph of double pancake A of coil 3 is plotted again with its smoothed graph. All the date that is smoothed, is averaged. Everything about the smoothing is more detailed explained in appendix D.

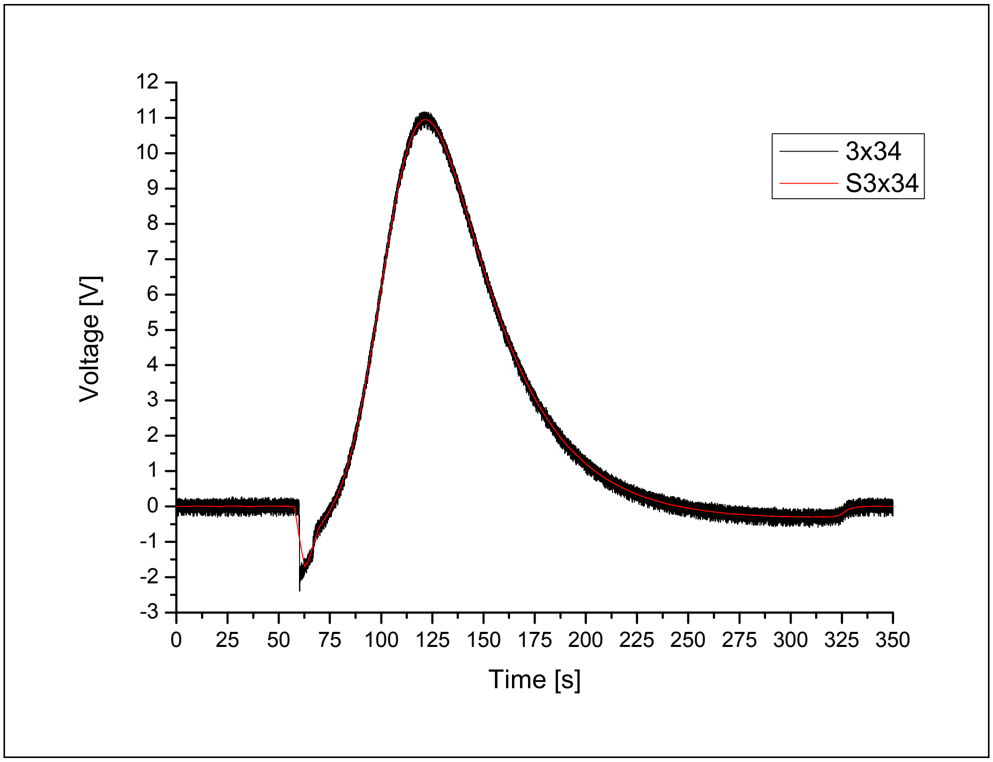

Figure 6.2: *Measured (black) and smoothed (red) voltage over double pancake A in coil 3.*

The current through the BT is shown in the next figure. This graph also had to be smoothed for further calculations.

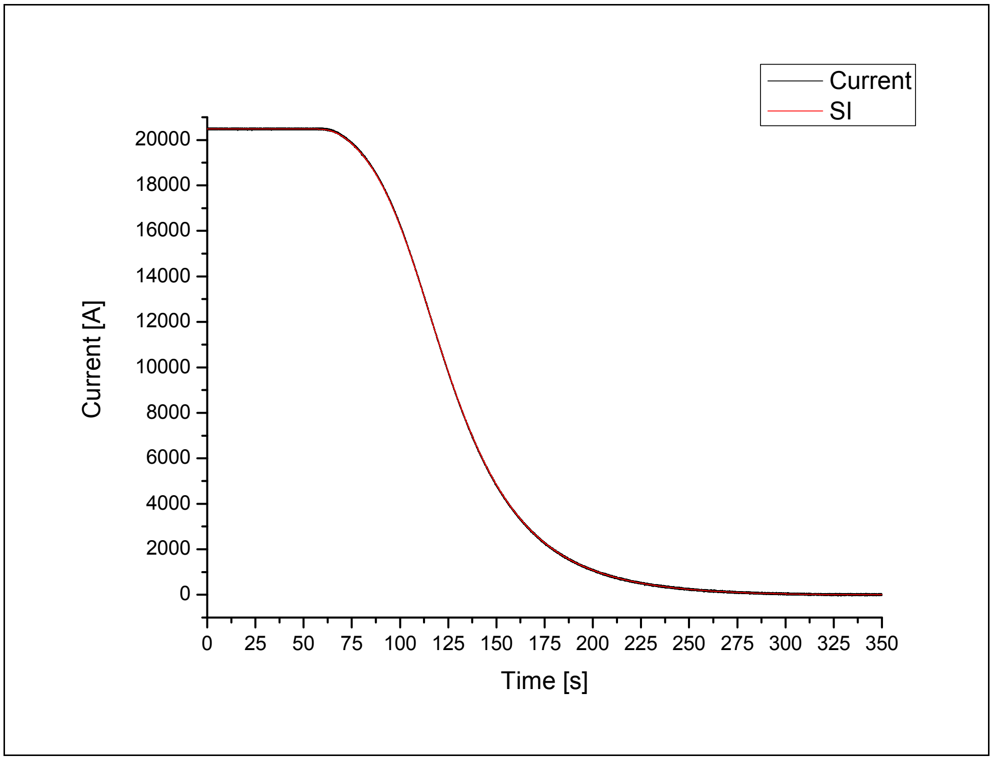

Figure 6.3: *Measured (black) and smoothed (red) current through BT.*

For the calculations, the derivative of the current had to be calculated. The smoothed current is differentiated and shown in figure 6.4. The signal became noisy and so again smoothing was applied.

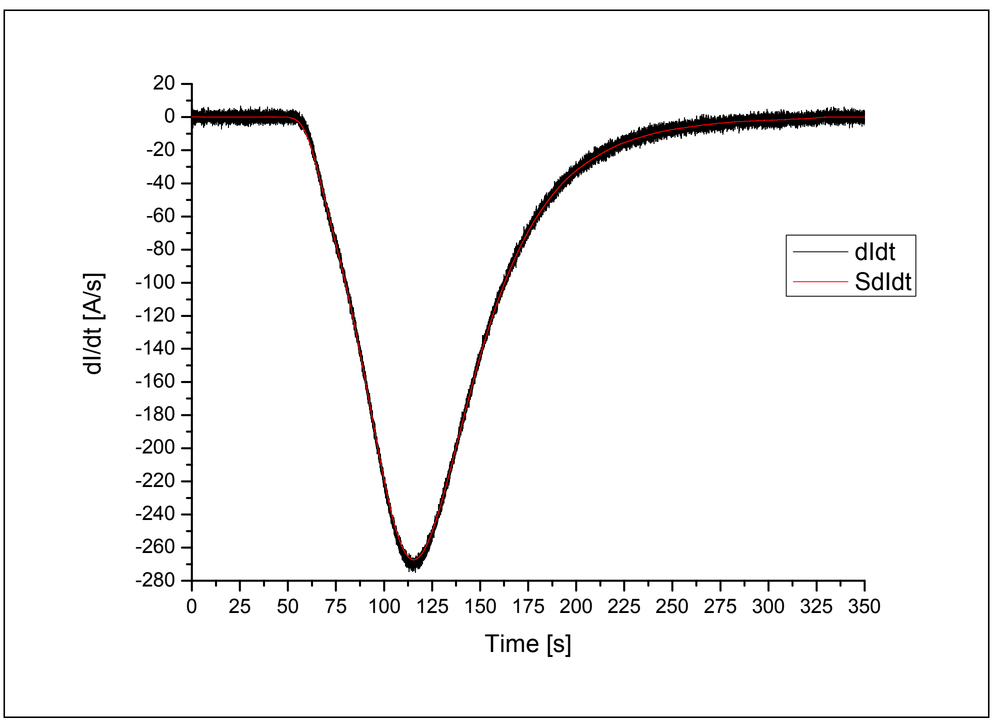

Figure 6.4: *Calculated (black) and smoothed (red) derivative of current.*

With the smoothed voltage and the smoothed derivative of the current, the resistive voltage of every pancake can be calculated (see formula 15). For pancake A of coil 3 the resistive part of the voltage is shown.

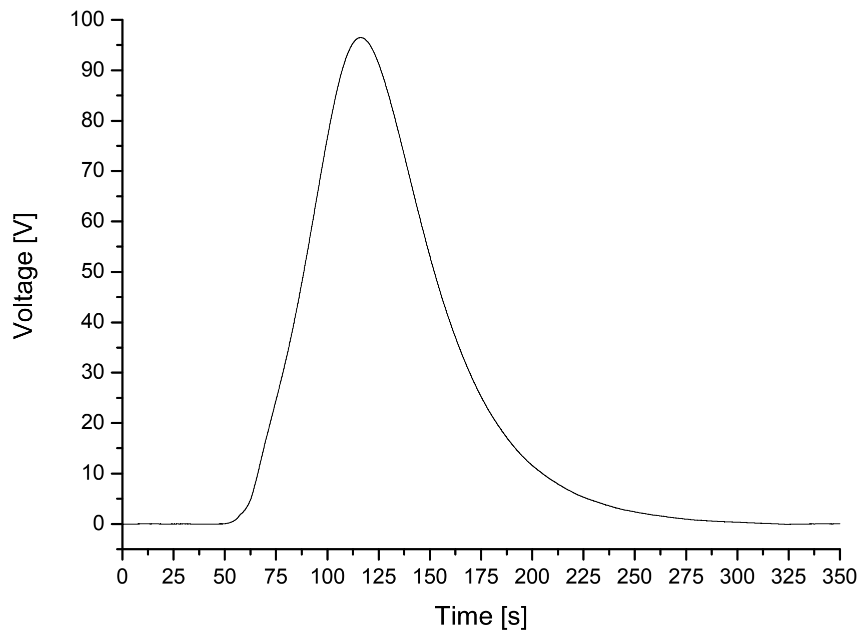

Figure 6.5: *Resistive voltage of double pancake A in coil 3.*

When this resistive voltage is divided by the smoothed current, the result is the resistance of the pancake as function of the time.

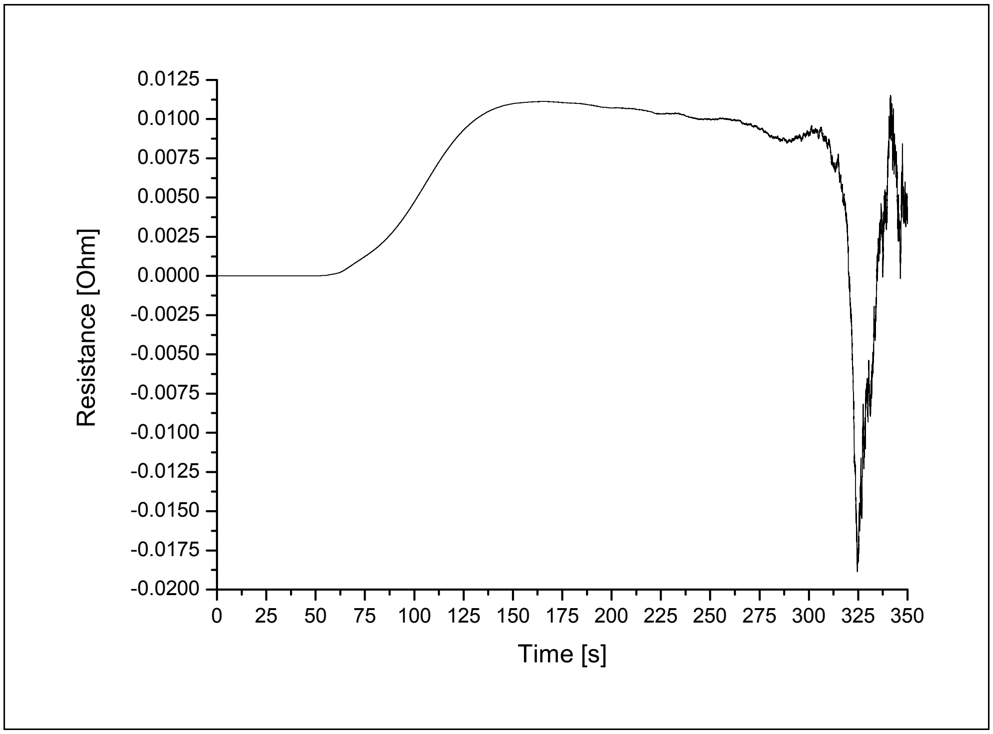

Figure 6.6: *Resistance of double pancake A in coil 3.*

The function of the resistance gets very noisy after 250 seconds, because the current is going to zero. This part of the graph is not important for the calculations.

The maximum resistance for face A in coil 3 is 0.01113Ω. The conductor has an area of 674.5 mm^2 and the average length of one turn in a pancake is 56.3 m.[3] In a double pancake, there are 2 pancakes with each 30 turns. With these properties, the resistivity can be calculated:

$$\rho = \frac{R \cdot A}{l} = \frac{0.01113 \cdot 674.5 \cdot 10^{-6}}{2 \cdot 30 \cdot 56.3} = 2.222 \cdot 10^{-9}\ \Omega\text{m} = 2.222\ \text{n}\Omega\cdot\text{m}.$$

In appendix E the information about the materials can be found. In case of a fast dump of the BT, it is assumed that the aluminium has a RRR (residual resistance ratio) of 1500 and a magnetic field around 1T.

The resistivity of 2.222 nΩ·m means that the aluminium has a temperature of 77.6K and an enthalpy of 8520.7 J/kg (appendix E.1). On this way, all the double pancake temperatures of the BT are estimated. These are showed in table 6.7:

Table 6.7: *Results of calculations on temperatures.*

Coil - double pancake	R_{max} [Ω]	Resistivity [nΩ·m]	T_{max} [K]
1 - 12 / B	0.00981	1.959	74.6
1 - 34 / A	0.00962	1.921	74.2
2 - 12 / B	0.00967	1.931	74.2
2 - 34 / A	0.01039	2.075	76.0
3 - 12 / B	0.01151	2.298	78.4
3 - 34 / A	0.01113	2.222	77.6
4 - 12 / B	0.01083	2.162	77.0
4 - 34 / A	0.00848	1.693	71.4
5 - 12 / B	0.00852	1.701	71.4
5 - 34 / A	0.00998	1.993	75.0
6 - 12 / B	0.01053	2.103	76.2
6 - 34 / A	0.00844	1.685	71.2
7 - 12 / B	0.00879	1.755	72.2
7 - 34 / A	0.00815	1.627	70.4
8 - 12 / B	0.00860	1.717	71.6
8 - 34 / A	0.00817	1.631	70.6

By the assumption that the temperature of the copper and the insulation is also 77.6K, the enthalpy of these parts is also known. For copper the value 5456.3 J/kg was found and for the insulation 9664.5 J/kg.

Now, with the enthalpy, the density and the volume[(3)] of the 3 components, the energies can be calculated:

Aluminium: $8520.7 \cdot 2698 \cdot 2.1349 = 49.1\,\text{MJ}$

Copper: $5456.3 \cdot 8960 \cdot 0.1436 = 7.0\,\text{MJ}$

Insulation: $9664.5 \cdot 1948 \cdot 0.2975 = 5.6\,\text{MJ}$

The temperature of the casing of double pancake 3A was at t_{max} was 35.1K. At this temperature the aluminium has an enthalpy of 440 J/kg. The casing of one coil is 6.8 m^3, so half can be seen as the casing of one double pancake. With this information, the stored energy in the casing can be calculated:

Casing: $440 \cdot 2698 \cdot 3.4 = 4.0\,\text{MJ}$

In the table underneath an overview of the results for all the pancakes is given. In the table there is a column H_{coil}, which is the sum of H_{Al}, H_{Cu} and $H_{insulation}$.

Table 6.8: *Results of calculations on enthalpy changes.*

Coil - double pancake	H_{Al} [MJ]	H_{Cu} [MJ]	$H_{insulation}$ [MJ]	H_{coil} [MJ]	T_{casing} [K]	H_{casing} [MJ]
1 - 12 / B	43.4	6.3	5.1	54.8	34.7	3.8
1 - 34 / A	42.6	6.2	5.1	53.9	34.4	3.8
2 - 12 / B	42.6	6.2	5.1	53.9	34.9	3.9
2 - 34 / A	46.0	6.6	5.3	57.9	35.1	4.0
3 - 12 / B	50.6	7.2	5.7	63.6	35.0	4.0
3 - 34 / A	49.1	7.0	5.6	61.7	35.1	4.0
4 - 12 / B	47.9	6.9	5.5	60.2	34.6	3.8
4 - 34 / A	37.7	5.5	4.6	47.8	33.0	3.2
5 - 12 / B	37.7	5.5	4.6	47.8	35.0	4.0
5 - 34 / A	44.1	6.4	5.2	55.7	36.4	4.7
6 - 12 / B	46.4	6.7	5.4	58.4	35.1	4.0
6 - 34 / A	37.3	5.5	4.6	47.4	35.2	4.1
7 - 12 / B	39.1	5.7	4.8	49.5	34.9	3.9
7 - 34 / A	35.9	5.3	4.5	45.7	35.0	4.0
8 - 12 / B	38.0	5.6	4.7	48.3	33.3	3.2
8 - 34 / A	36.3	5.3	4.5	46.2	35.0	4.0
Total:	674.6	97.9	80.3	852.8		62.9

With these enthalpy changes, equation 13b is almost complete:

$$E_{cable} = 65.7 + E_{undefined} = 49.1 + 7.0 + 5.6 + 4.0 + E_{undefined}$$

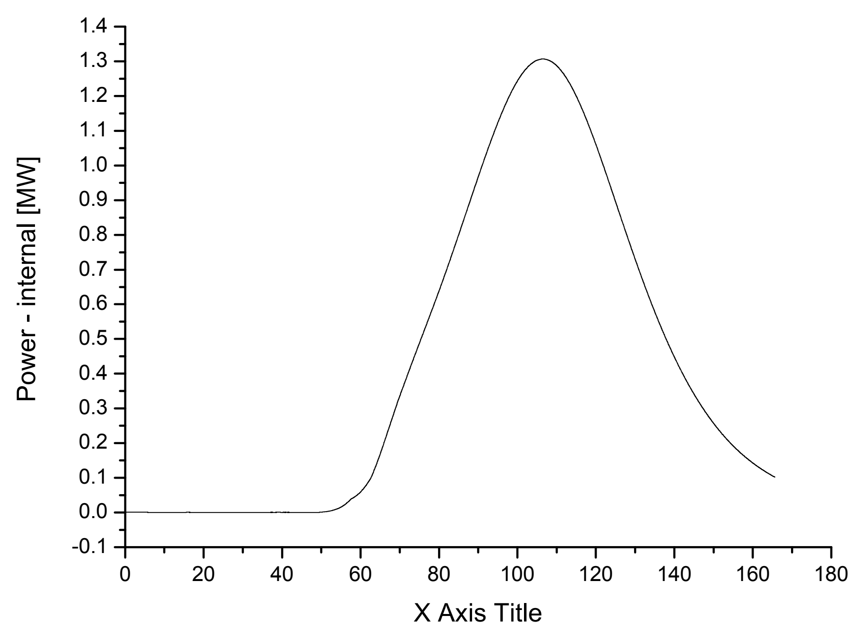

Figure 6.9: *Power in double pancake A in coil 3.*

The smoothed graphs of the current (figure 6.3) and the resistive voltage (figure 6.5) are multiplied (figure 6.9). Note that the graph ends at moment t_{max}. The integration gives a result of 71.7 MJ. After t_{max} almost no heat is generated anymore in the double pancake, so the temperature will decrease again. The heat that is generated after t_{max}, will flow to the surrounding material of the double pancake.

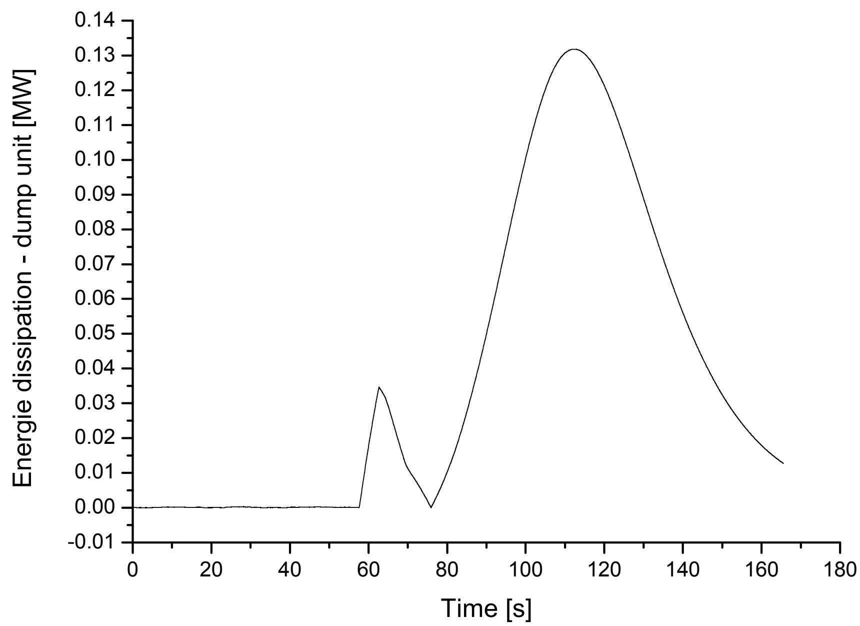

Figure 6.10: *Energy dissipation in dump unit, contribution of double pancake A in coil 3.*

The contribution of the double pancake A in coil 3 to the energy dissipation in the dump unit is showed in figure 6.10. After integration of this graph and also of the 15 other graphs of the rest of the BT, the total energy dissipated in the dump unit can be calculated. When the total energy is divided by 16, then the energy in dump unit of equation 13a is known, which is 2.0 MJ. Now equation 13a and 13b are complete and the last variables can be calculated:

$$E_{tot} = 71.7 + 2.0 \rightarrow E_{tot} = 73.7$$

$$71.7 = 65.7 + E_{undefined} = 49.1 + 7.0 + 5.6 + 4.0 + E_{undefined} \rightarrow E_{undefined} = 6.0$$

The total theoretical energy dissipated from the double pancake A in coil 3 until t_{max} can be calculated by formula 7:

$$E_{tot,th} = \frac{1}{2} L\left(I_i^{\,2} - I_f^{\,2}\right) = \frac{1}{2} 5.1416\left(20483^2 - 2898^2\right) = 66.1\text{MJ}$$

This difference ($73.7 - 66.1 = 7.6$ MJ) seems very big, but this is only one double pancake. In table 6.11 the results of the calculations for all the double pancakes can be found. When the total energies of all double pancakes are summed, then the difference is only $(1022.4 + 32.6) - 1053.4 = 1.6$ MJ, which is almost nothing.

Table 6.11: *Results of calculations on energies.*

Coil - double pancake	$E_{tot,th}$ [MJ]	E_{cable} [MJ]	H_{cable} [MJ]	$E_{undefined}$ [MJ]	E_{dump} [MJ]
1 - 12 / B	66.1	63.1	58.6	4.4	2.0
1 - 34 / A	66.1	63.3	57.6	5.7	2.0
2 - 12 / B	65.3	65.5	57.8	7.7	2.0
2 - 34 / A	65.8	69.7	62.0	7.7	2.0
3 - 12 / B	66.1	73.2	67.6	5.5	2.0
3 - 34 / A	65.9	71.7	65.7	6.0	2.0
4 - 12 / B	65.9	70.6	64.1	6.6	2.0
4 - 34 / A	65.8	58.4	51.0	7.4	2.0
5 - 12 / B	65.8	58.6	51.9	6.7	2.0
5 - 34 / A	65.8	66.5	60.4	6.1	2.0
6 - 12 / B	65.8	69.6	62.4	7.2	2.0
6 - 34 / A	65.8	59.1	51.6	7.5	2.0
7 - 12 / B	65.9	59.1	53.5	5.6	2.0
7 - 34 / A	65.8	57.4	49.8	7.6	2.0
8 - 12 / B	65.6	59.7	51.5	8.2	2.0
8 - 34 / A	65.6	56.8	50.2	6.6	2.0
Total:	1053.4	1022.4	915.7	106.7	32.6

The equations 13a and 13b can also be made for the whole BT:

$$E_{tot} = E_{cable} + E_{dump}$$

$$1055.0 = 1022.4 + 32.6 \text{ MJ}$$

$$E_{cable} = H_{cable} + E_{undefined} = H_{Al} + H_{Cu} + H_{insulation} + H_{casing} + E_{undefined}$$

$$1022.4 = 915.7 + 106.7 = 674.6 + 97.9 + 80.3 + 62.9 + 106.7 \text{ MJ}$$

For the ECTs the energy distribution could not be calculated correctly. The energy in one end-cap is (only measurements available till 10 kA):

$$E = \frac{1}{2} \cdot 1 \cdot 10000^2 = 50 \text{ MJ}$$

This energy has to be divided by 16, because the energy dissipation is calculated for each double pancake. Then the energy is a little bit more then 3 MJ, which is not enough. The calculations are not precise enough to get good results in this case.

6.3 Results

In figure 6.12 an overview of the energy dissipation is given for double pancake A in coil 3 of the BT.

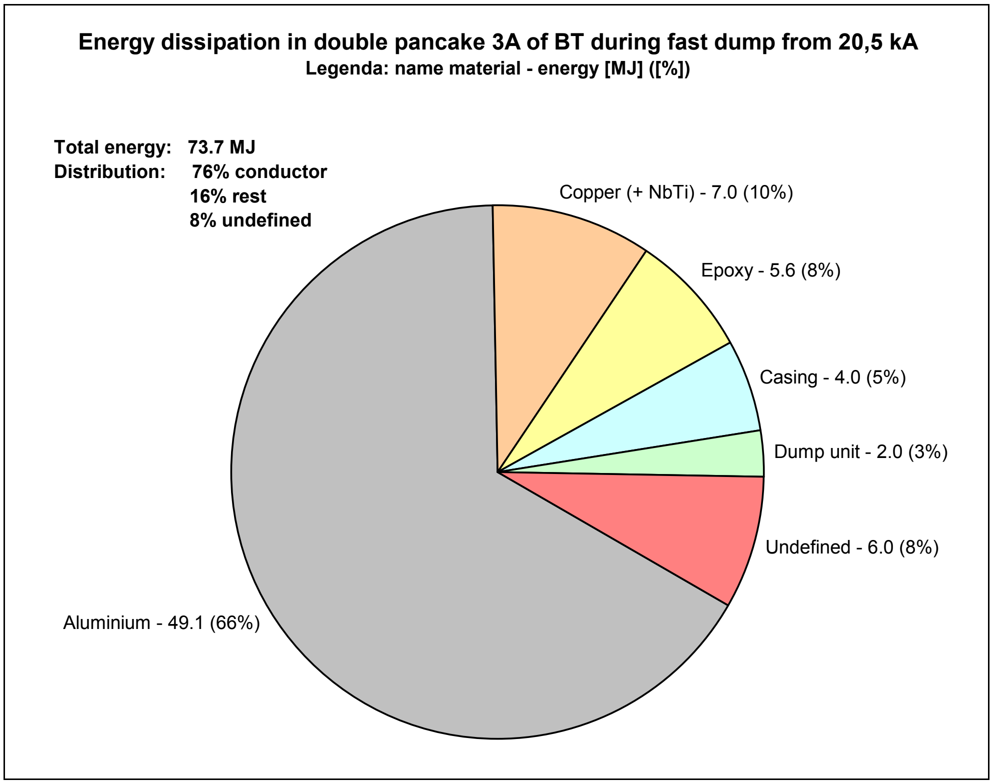

Figure 6.12: *Energy distribution in double pancake A in coil 3.*

The conductor consists of the aluminium and the copper part. In the graph of figure 6.13 the energy distribution is shown of the whole BT.

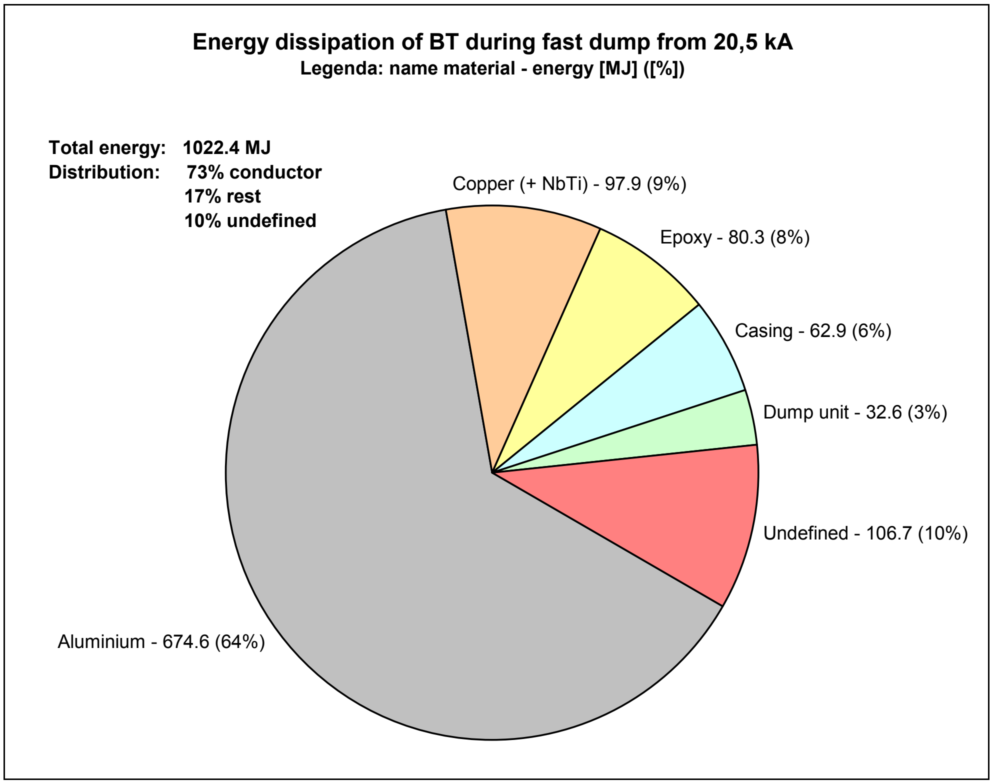

Figure 6.13: *Energy distribution in BT.*

The graphs for the double pancake 3A and the whole BT are pretty similar in terms of percentages. In case of the BT, the energy distribution is calculated with 10% of accuracy. For the cover plates of the casing it is not calculated what the stored energy could be. They are made of aluminium and the temperature is maybe higher than the casing, because their mass is less and they are placed against the double pancakes. Also the casing does not have a uniform temperature. One must keep in mind that a part of the uncertainties are also within this undefined part.

In the conductor itself, 73% of the total energy is stored after the fast dump. The remaining 17% was stored in the isolation, the casing and the dump unit. During the slow dump, (almost) all the energy is dissipated in the dump unit, but during the fast dump, the unit has almost no role in the energy dissipation.

Another conclusion drawn from these results is that the aluminium stabiliser of the cable has a big influence on the discharge during the fast dump. 64% of the energy goes in the aluminium. This can be explained by the high specific heat of aluminium. When another material would be used, the temperature after a fast dump would be higher, to store the same energy.

7 Residual resistance ratio

In this chapter the relation between the residual resistance ratio of the double pancakes and the quench properties is investigated. First this ratio has to be estimated for the BT and ECTs. Then there will be searched for a correlation to the maximum temperature and the start time of a quench.

7.1 Theory

The residual resistance ratio (RRR) of a metal wire is defined as follows:

$$RRR = \frac{R_{300\text{K}}}{R_{4.2\text{K}}} \tag{17}$$

The ratio can be calculated by dividing the resistance of the wire at room temperature, 300K, by the resistance at the temperature of boiling Helium, 4.2K. Assuming a constant resistance at 300K, then a higher RRR means a smaller resistance at 4.2K. When a wire is superconducting at 4.2K then the critical temperature will be used. Above this critical temperature the wire is not superconducting anymore and has it the lowest resistance.

In the graph underneath one can see some implementations for an aluminium wire. The graph shows the resistivity versus the temperature. These values are extracted from the program Cryocomp of the company Cryodata Inc.[(5)]. The properties that were used are 500, 1000 and 1500 as RRR and a magnetic field of 0, 1 and 2 T.

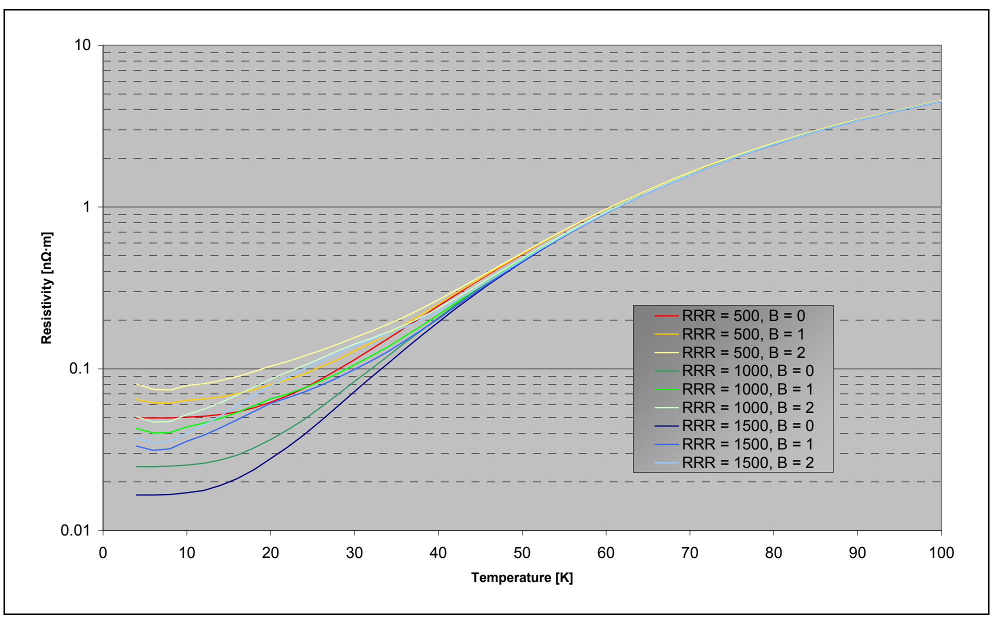

Figure 7.1: *Resistance dependence on RRR and magnetic field.*

As one can see in the graph above, the resistance is almost not dependent on the RRR and the magnetic field, when the temperature is higher then

50K. At 300K the resistance of the wire is the same in a magnetic field of 0 or 2 T. But the resistances of the wire of a RRR of 500 and a wire with a RRR of 1500 do not differ more than 4%.

When one coil would have a lower RRR with respect to the other coils, then a few consequences can be expected. Since a lower RRR means that the resistance at low temperature is higher, more energy will be dissipated in this coil during the fast dump. This will make the coil rise more in temperature than the other coils.

There will also be investigated if the RRR has something to do with the time in which a coil leaves the superconducting state during a fast dump.

7.2 Methods

It is assumed that the resistivity of aluminium at room temperature, 26 nΩ·m is. With formula (16) one gets the resistance for a double pancake in an ECT:

$$R = \frac{l \cdot \rho}{A} = 2\frac{29 \cdot 14 \cdot 26 \cdot 10^{-9}}{492 \cdot 10^{-6}} = 42.9\,\text{m}\Omega^{(4)}$$

7.2.1 Fast dump

In the calculation of the energy dissipation, there is explained how to get the resistance versus time during the fast dump, using the voltage and the current of the pancakes. In figure 7.2 one can see the graph of the behaviour of the resistance as function of the temperature of a superconductor in general. For every wire with different properties or dimensions, the graph is different, but the shape is always the same.

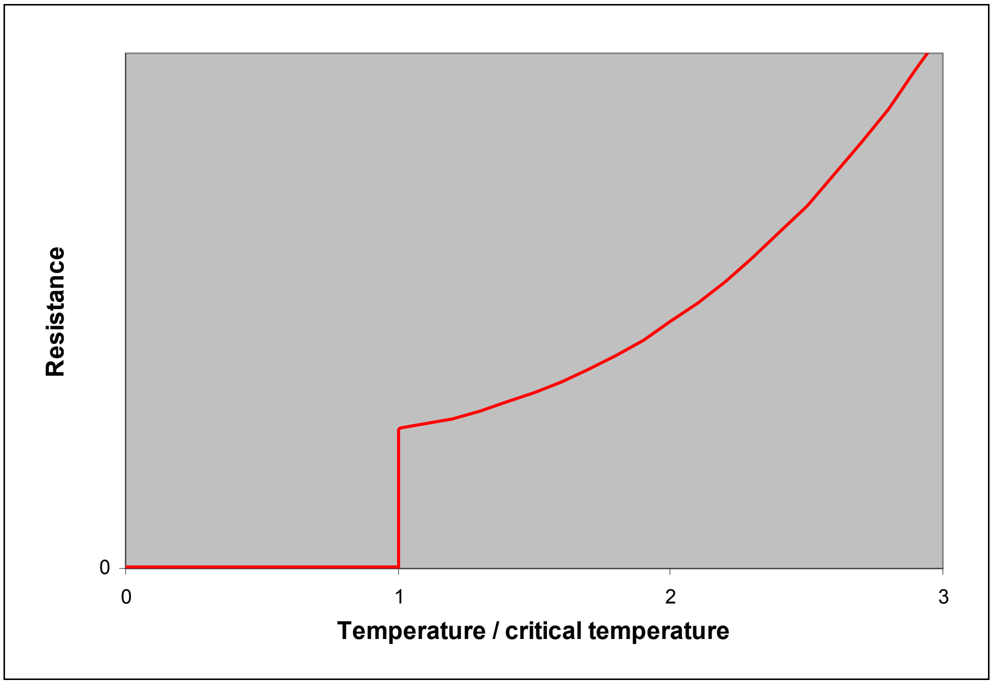

Figure 7.2: *Typical behaviour of resistance of superconducting wire.*

The transition at the critical temperature can also be seen in the graph of the resistance of the cable during the fast dump. The superconducting material used in the toroid magnets has a critical temperature of 9.2K. The resistance at this point will be used to calculate the RRR.

7.2.2 Resistance measurement

Another method to estimate the resistance at the critical temperature is to measure the resistance at a very low temperature (10-15K). At these temperatures is the resistance does not change that much. There can be assumed that the resistance does not change at all, then this value can be used to calculate the RRR.

7.3 Measurements

7.3.1 Barrel Toroid

During the manufacturing of the BT coils, tests are done to measure the RRR of the double pancakes. (There are no measurements done yet after the coils where in their final configuration.) The results of the measurements are listed underneath. The maximum temperature is also put in the table. This temperature is the maximum temperature calculated in previous chapter.

Table 7.3: *Results of RRR measurements on double pancakes of BT.*

Coil - double pancake	RRR [-]	T_{max} [K]
1 - A	2500	74.2
1 - B	1400	74.6
2 - A	1778	76.0
2 - B	1455	74.2
3 - A	1130	77.6
3 - B	1284	78.4
4 - A	3058	71.4
4 - B	1511	77.0
5 - A	1535	75.0
5 - B	1822	71.4
6 - A	1969	71.2
6 - B	1519	76.2
7 - A	2296	70.4
7 - B	2402	72.2
8 - A	2824	70.6
8 - B	2093	71.6

When the maximum temperature is plotted against the RRR, then a trend can be seen. A double pancake with a relative low RRR has a relatively higher maximum temperature, as expected and explained in the first paragraph.

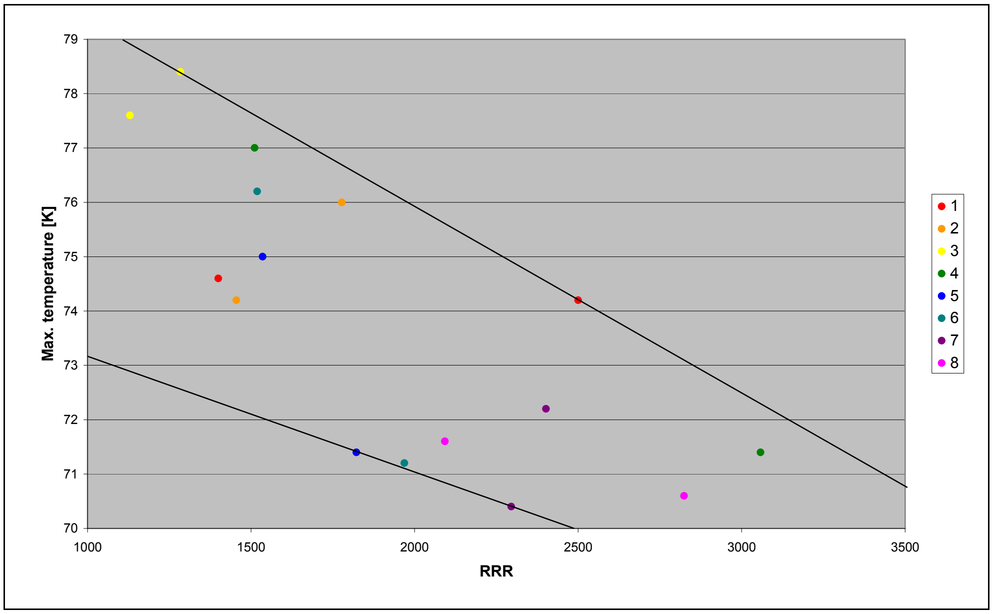

Figure 7.4: *Relation between RRR and maximum temperature.*

7.3.2 End-Cap Toroids

The following results were derived from the measurements of a fast-dump from 10kA for both the ECTs. With the same method as in previous chapter, the following graphs of the resistances are found.

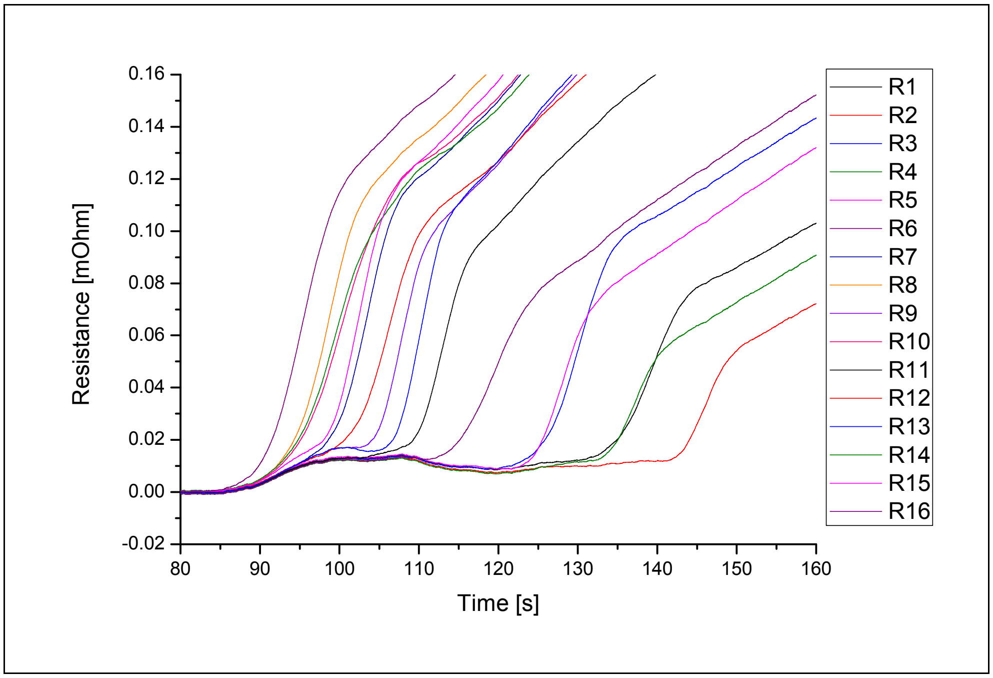

Figure 7.5: *Resistances of ECT A during fast dump (10kA).*

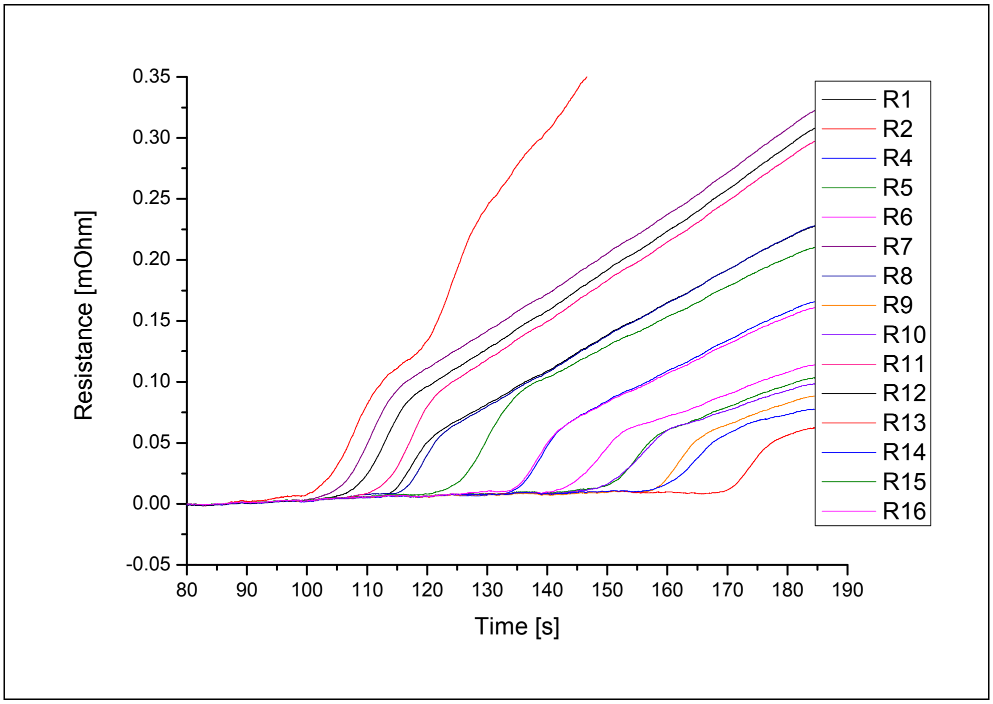

Figure 7.6: *Resistances of ECT C during fast dump (10kA).*

Note: The voltage in ECT C of double pancake B in coil 1 and double pancake A in coil 2 are measured together as some voltage taps were lost during assembly. The calculated resistance from this voltage is shown as R2 in the graph and R3 is not defined. The graph in figure 7.2 can be recognized in the graphs of 7.5 and 7.6. During other tests of BT and ECTs the energies were too high to get the same graphs as above. When the energy is too high, the transition process goes so fast that it can not be seen.

The resistances of ECT A and C at the bending point are listed in table 7.7.

Table 7.7: *Results for resistances for RRR measurements.*

Coil - double pancake	resistance [Ω]	
	ECT A	ECT C
1 - A	0.0000753	0.0000565
1 - B	0.0000538	0.0000950
2 - A	0.0000934	0.0000970
2 - B	0.0000550	0.0000578
3 - A	0.0000751	0.0000560
3 - B	0.0000806	0.0000564
4 - A	0.0001082	0.0000870
4 - B	0.0001055	0.0000566
5 - A	0.0000949	0.0000589
5 - B	0.0001057	0.0000591
6 - A	0.0000875	0.0000863
6 - B	0.0000986	0.0000792
7 - A	0.0000995	0.0000534
7 - B	0.0000987	0.0000518
8 - A	0.0001096	0.0000836
8 - B	0.0000869	0.0000556

To calculate the RRR (double pancake 1A of ECT A) we use formula 17:

$$RRR = \frac{0.0429}{0.0000753} = 570$$

(The resistance 0.0429 Ω was calculated in the beginning of paragraph 7.2.) In the tables 7.8 and 7.9 the results for RRR can be found for respectively ECT A and C.

Table 7.8: *Results of RRR measurements on double pancakes of ECT A.*

Coil - double pancake	RRR [-]					t_{start}
	FD	M1	M2	M3	M4	[K]
1 - A	570	1023	1773	1950	1650	74
1 - B	797	1300	2509	2681	2145	82
2 - A	459	784	1324	1430	1192	64
2 - B	780	1193	2480	2860	2145	74
3 - A	571	926	1915	2145	1716	64
3 - B	532	917	1898	2043	1650	54
4 - A	396	695	1114	1192	1021	38
4 - B	407	698	1123	1192	1021	33
5 - A	452	842	1358	1430	1226	44
5 - B	406	834	1336	1430	1226	35
6 - A	490	919	1469	1532	1341	49
6 - B	435	864	1358	1430	1262	41
7 - A	431	803	1202	1262	1100	46
7 - B	435	935	1469	1589	1341	34
8 - A	392	784	1195	1226	1021	38
8 - B	494	775	1169	1226	1021	30

Table 7.9: *Results of RRR measurements on double pancakes of ECT C.*

Coil - double pancake	RRR [-]					t_{start}
	FD	M1	M2	M3	M4	[K]
1 - A	759	1318	2648	3064	2383	53
1 - B	452	841	1437	1560	1320	43
2 - A	442	841	1437	1560	1320	61
2 - B	742	1081	2223	2524	1950	74
3 - A	766	1071	2538	2860	2258	90
3 - B	761	1053	2509	2860	2258	83
4 - A	493	781	1349	1479	1226	42
4 - B	758	1147	2466	2860	2145	55
5 - A	728	1281	2584	2860	2258	98
5 - B	726	1262	2524	2860	2258	89
6 - A	497	932	1571	1650	1430	50
6 - B	542	960	1650	1716	1532	44
7 - A	803	1435	3109	3300	2681	110
7 - B	828	1298	3000	3300	2681	99
8 - A	513	973	1637	1716	1532	63
8 - B	772	1286	2494	2681	2258	74

In the tables, FD stands for the method using the fast dump data and M stands for the measurements. During the measurement the resistance was measured at a low temperature. The measurement conditions were (temperature is averaged):

Table 7.10: *Measurement conditions.*

Measurement	T [K]	I [A]
1	20	20
2	11	100
3	10	100
4	13	100

In the tables also the start time of the quench is presented. This will be discussed a little bit further on. All the values for the RRR from the table are plotted in the figures 7.11 and 7.12.

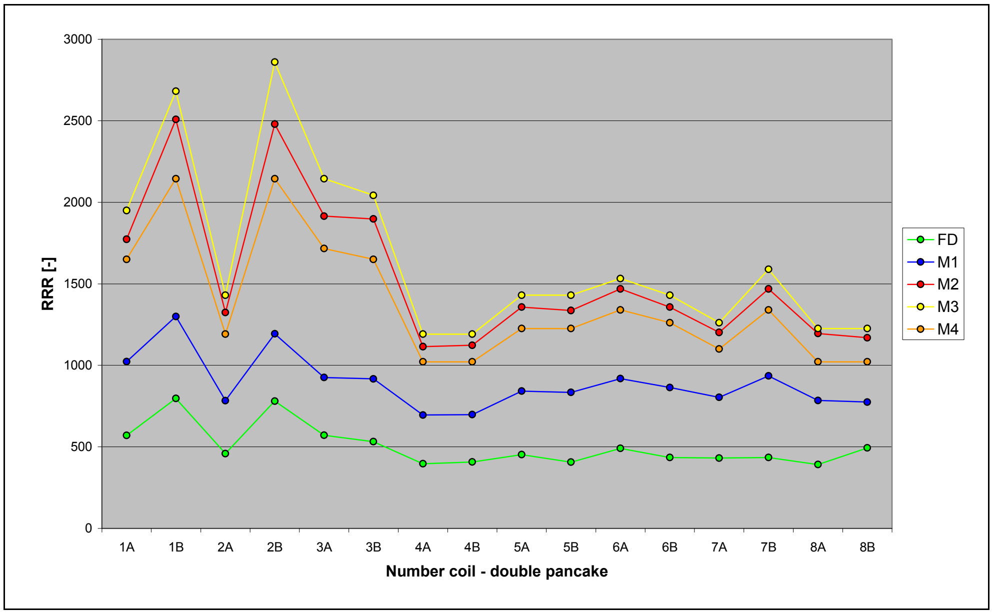

Figure 7.11: *RRR of ECT A for different methods.*

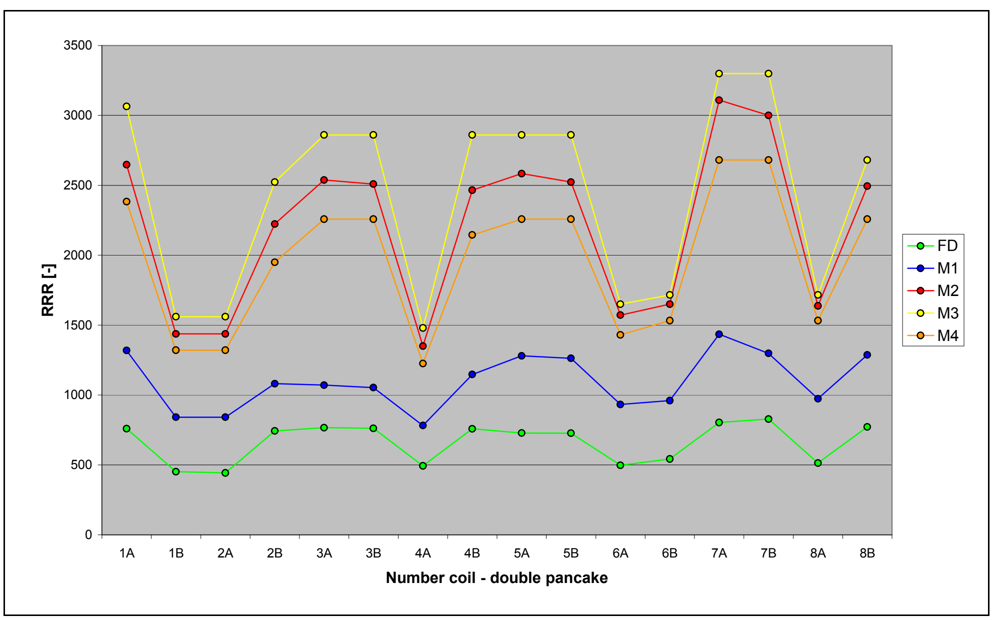

Figure 7.12: *RRR of ECT C for different methods.*

One can clearly see that relatively all measurement are the same, for both ECTs, besides some exceptions. The explanation why the absolute values differ that much, is because the measurement conditions were very different. The temperature of the conductor and the magnetic field where it is in, influence the resistance a lot. During the fast dump there was a magnetic field of 1T. During the measurements the field was approximately zero. The temperature during the first measurement was 20K and the resistance was already very high. That is why the RRR for this test are so high. Measurement 2 was the most precise measurement (in its condition), so that one is used to plot the start time of the quench against the RRR in figure 7.13. A distinction has been made whether the double pancake quenched first or as second in a coil.

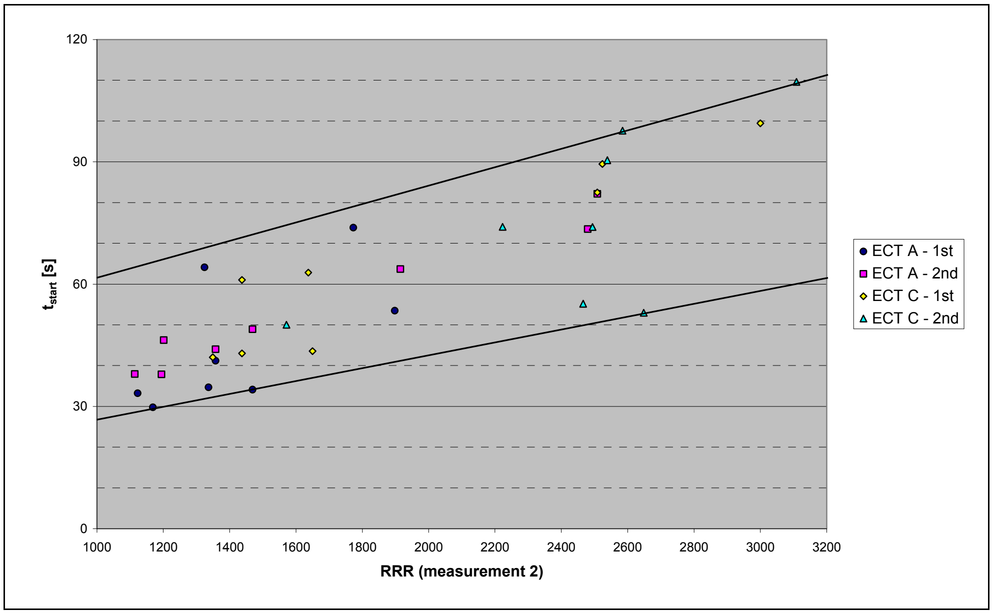

Figure 7.13: *Start time of quench as function of RRR.*

The trend that a higher RRR means a later start of the quench can be clearly seen. An explanation could be that the high RRR means a low resistance at low temperatures and so it will take longer before the coil leaves the superconducting state.

7.4 Conclusion

From the calculations of the Barrel Toroid it appeared that a double pancake with a relative low RRR has a relatively higher maximum temperature, as expected.

For both ECTs, the RRR is measured and calculated for all the double pancakes. The ECTs also showed that a double pancake quenched later, when it has a higher RRR with respect to other double pancakes.

8 Conclusion

The goal was to make simulations of the electrical behaviour of the magnet system during a slow dump. In this way, an explanation has been found for the start phenomenon of the slow dump of the Barrel Toroidal magnet of the ATLAS detector. Some extra analyses on the measurements are performed to describe the energy dissipation during a fast dump. Also a correlation between the RRR of the conductor and the properties of the quench is found.

The results of the simulation of the Barrel Toroid as one coil were as expected. The simulation is correct and precise enough to reproduce the measurements. This simulation was extended to a simulation of the eight coils separately. The result was that a change up to 4% in the resistance of the coil casing can be the cause of the difference in the coil voltages in the beginning of the slow dump.

The calculations of the energy dissipation during a fast dump of the BT showed that 73% of the energy was stored in the conductor. The aluminium in the conductor stored 64% of this energy and 17% was stored in the isolation, the casing and the dump unit. Not for all the parts of the magnet the change in enthalpy is calculated. An undefined 10% of the energy is also due to the inaccuracy of the calculations.

By analysing a fast dump measurement of the Barrel Toroid, it appeared that a double pancake with a relative low RRR has a relatively higher maximum temperature after the dump, as expected. For both ECTs, the RRR is measured and calculated for all the double pancakes. The ECTs showed that a double pancake quenched later, when it has a higher value for the RRR with respect to other double pancakes.

9 References

General information

(1) *http://www.cern.ch/*
CERN, DSU-CO, 2008

Properties magnet system

(2) *Magnet Project Technical Design Report Volume 1: Magnet system*
Prepared by ATLAS/Magnet Project Collaboration/CERN-ATLAS team, 30 April 1997
Reference ATLAS TDR 6; CERN/LHCC 97-18, Issue 1, Revision 0

(3) *Barrel Toroid: Magnet Project Technical Design Report Volume 2*
Prepared by ATLAS/Magnet Project Collaboration/Barrel Toroid Group, 30 April 1997
Reference ATLAS TDR-7; CERN/LHCC 97-19, Issue 1, Revision 0

(4) *End-Cap Toroids: Magnet Project Technical Design Report Volume 3*
Prepared by ATLAS/Magnet Project Collaboration/End-Cap Toroid Group, 30 April 1997
Reference ATLAS TDR-8; CERN/LHCC 97-20, Issue 1, Revision 0

Appendix

A Overview properties magnet system ATLAS

A.1 General properties

Property	unit	Barrel Toroid	1 End-Cap Toroid
Overall dimensions			
Inner diameter	m	9.4	1.65
Outer diameter	m	20.1	10.7
Axial length	m	25.3	5
Number of coils	-	8	8
Weight:			
Conductor	10^3 kg	118	20.5
Cold mass	10^3 kg	370	160
Total assembly	10^3 kg	830	239
Coils:			
Number of turns per coil	-	120	116
Operating current	kA	20.5	20.5
Stored energy	MJ	1080	206
Peak field	T	3.9	4.1
Conductor (NbTi/Cu/Al):			
Overall size (w x h)	mm^2	57 x 12	41 x 12
Ratio Al : Cu : NbTi	- : - : -	28 : 1.3 : 1	19 : 1.3 : 1
Number of strands in cable	-	33	40
Strand diameter	mm	1.3	1.3
Total length	km	56.3	12.8

A.2 Electrical properties Barrel Toroid

Property	unit	1 coil	1 casing
Resistance	Ω	0	$14 \cdot 10^{-6}$
Self inductance	H	0.5382	$44 \cdot 10^{-6}$
Mutual inductance with 1 coil	H	-	$4.6 \cdot 10^{-3}$
Mutual inductance with 7 other coils	H	0.1045	$0.9 \cdot 10^{-3}$
Mutual inductance with 1 casing	H	$4.6 \cdot 10^{-3}$	-
Mutual inductance with 7 other casings	H	-	$8 \cdot 10^{-6}$

B Simulation of one coil

calculation properties

number of measurements [-] $\tau := 50000$

time between 2 measurements [s] $\Delta t := 0.2$

time of all measeurements [s] $\tau \cdot \Delta t = 1 \times 10^4$ counter $i := 0 .. \tau$

coil properties	<u>primary coil</u>	<u>secondary coil</u>
resistance [Ω]	$R_p := 0.001145$	$R_s := \frac{14 \cdot 10^{-6}}{8}$
inductance [H]	$L_p := 5.1416$	$L_s := \frac{52 \cdot 10^{-6}}{8}$
mutual inductance [H]	$M := \frac{5.5 \cdot 10^{-3}}{8}$	

measurement file

$D :=$

	0	1	2	3	4
0	1	$8.541 \cdot 10^3$	$8.549 \cdot 10^3$	6.401	-16.805
1	2	$8.554 \cdot 10^3$	$8.543 \cdot 10^3$	-5.809	5.175
2	3	$8.53 \cdot 10^3$	$8.534 \cdot 10^3$	-3.379	6.395
3	4	$8.542 \cdot 10^3$	$8.539 \cdot 10^3$	0.291	...

factor current [-] $A := 2.4$

factor voltage [-] $V := \frac{1}{1000} \cdot 10$

start time [s] $t_0 := 744$

total voltage primary coils [V] $U_T := V \left[\sum_{n=1}^{8} \left(D^{\langle 2n+1 \rangle} + D^{\langle 2 \cdot n+2 \rangle} \right) \right]$

initial values

voltage diode [V]

current primary coil [A]

current secondary coil [A]

$$\begin{pmatrix} U_{d_0} \\ I_{p_0} \\ I_{s_0} \end{pmatrix} := \begin{pmatrix} 10 \cdot 0.665 \\ A \cdot 8533 \\ 0 \end{pmatrix}$$

calculation of all values

$$\begin{pmatrix} U_{d_{i+1}} \\ I_{p_{i+1}} \\ I_{s_{i+1}} \end{pmatrix} := \begin{bmatrix} \text{if}\left[\left(I_{p_i} + \dfrac{-R_p \cdot I_{p_i} + \dfrac{M \cdot R_s}{L_s} \cdot I_{s_i} - U_{d_0}}{L_p - \dfrac{M^2}{L_s}} \cdot \Delta t\right) \le 0, \dfrac{M \cdot R_s}{L_s} \cdot I_{s_i}, U_{d_0}\right] \\ \text{if}\left[\left(I_{p_i} + \dfrac{-R_p \cdot I_{p_i} + \dfrac{M \cdot R_s}{L_s} \cdot I_{s_i} - U_{d_i}}{L_p - \dfrac{M^2}{L_s}} \cdot \Delta t\right) \le 0, 0, \left(I_{p_i} + \dfrac{-R_p \cdot I_{p_i} + \dfrac{M \cdot R_s}{L_s} \cdot I_{s_i} - U_{d_i}}{L_p - \dfrac{M^2}{L_s}} \cdot \Delta t\right)\right] \\ I_{s_i} + \left[\dfrac{M}{L_p \cdot L_s - M^2} \cdot \left(R_p \cdot I_{p_i} + U_{d_i}\right) - \dfrac{L_p \cdot R_s}{L_p \cdot L_s - M^2} \cdot I_{s_i}\right] \cdot \Delta t \end{bmatrix}$$

	<u>primary circuit</u>	<u>secondary circuit</u>
voltage resistance [V]	$U_{Rp_i} := R_p \cdot I_{p_i}$	$U_{Rs_i} := R_s \cdot I_{s_i}$
voltage coil [V]	$U_{Lp_i} := L_p \cdot \dfrac{I_{p_{i+1}} - I_{p_i}}{\Delta t} + M \cdot \dfrac{I_{s_{i+1}} - I_{s_i}}{\Delta t}$	$U_{Ls_i} := L_s \cdot \dfrac{I_{s_{i+1}} - I_{s_i}}{\Delta t} + M \cdot \dfrac{I_{p_{i+1}} - I_{p_i}}{\Delta t}$
power [W]	$P_{p_i} := \left\lvert U_{Rp_i} \cdot I_{p_i} \right\rvert + \left\lvert U_{d_i} \cdot I_{p_i} \right\rvert$	$P_{s_i} := \left\lvert U_{Rs_i} \cdot I_{s_i} \right\rvert$
total power [W]	$P_i := P_{p_i} + P_{s_i}$	

graph: calculated currents [A] versus time [s]

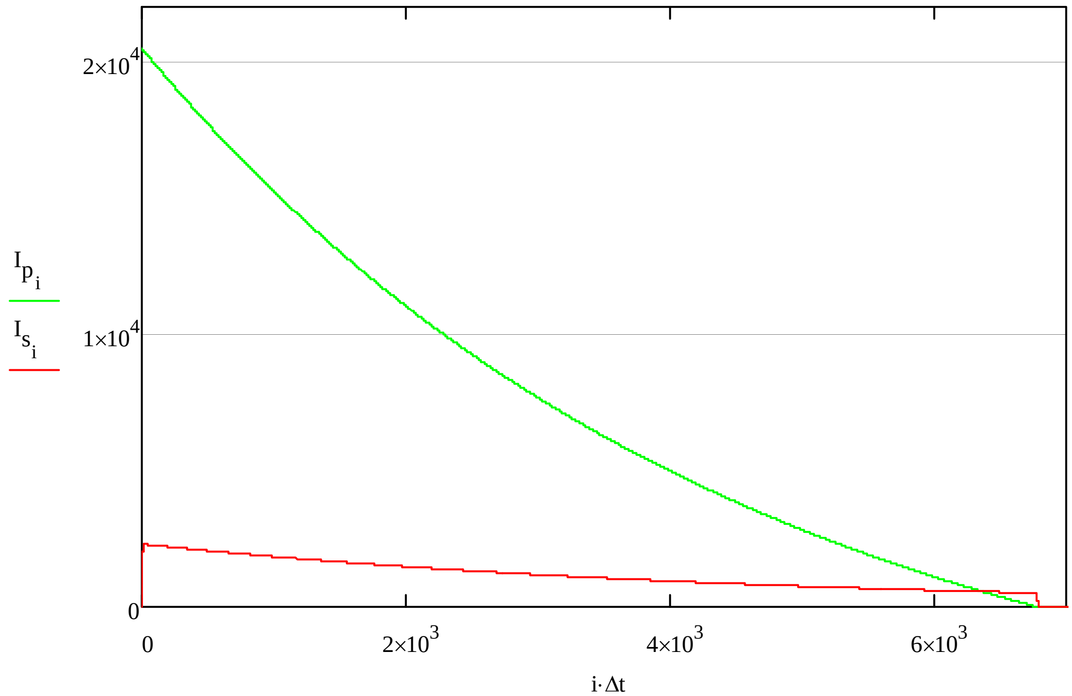

graph: calculated voltages in primary cicuit [V] versus time [s]

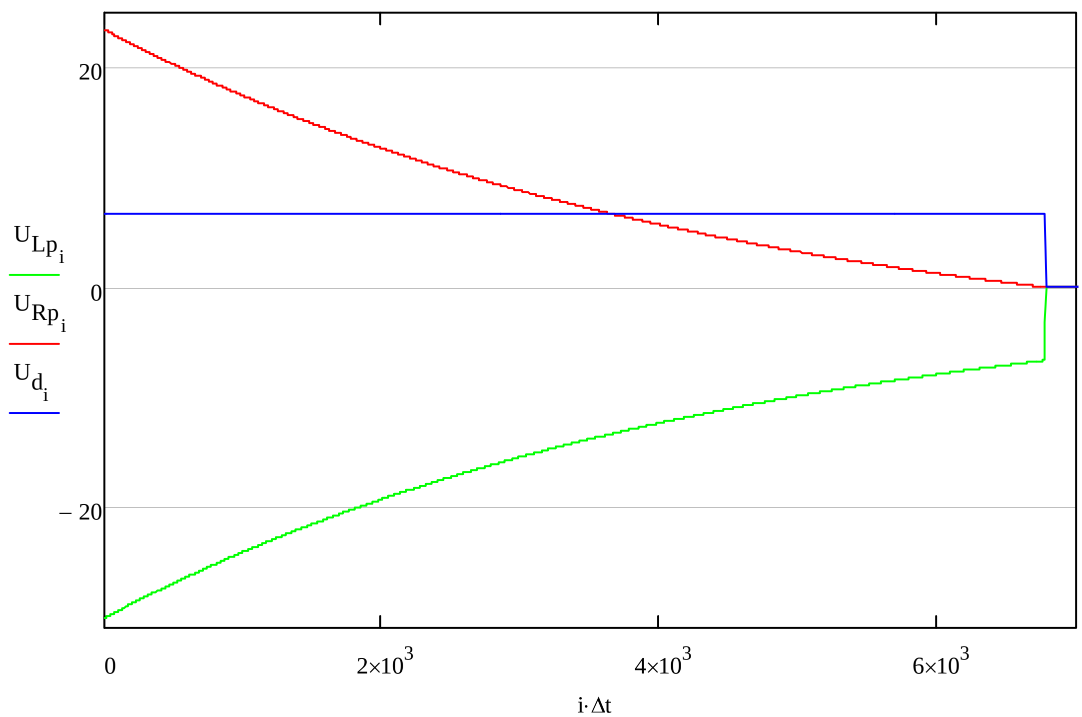

graph: power [W] versus time [s]
surface under graph: stored energy = 1.080·10⁹ [J]

$$\sum_i \left(P_i \cdot \Delta t\right) = 1.078\times 10^9$$

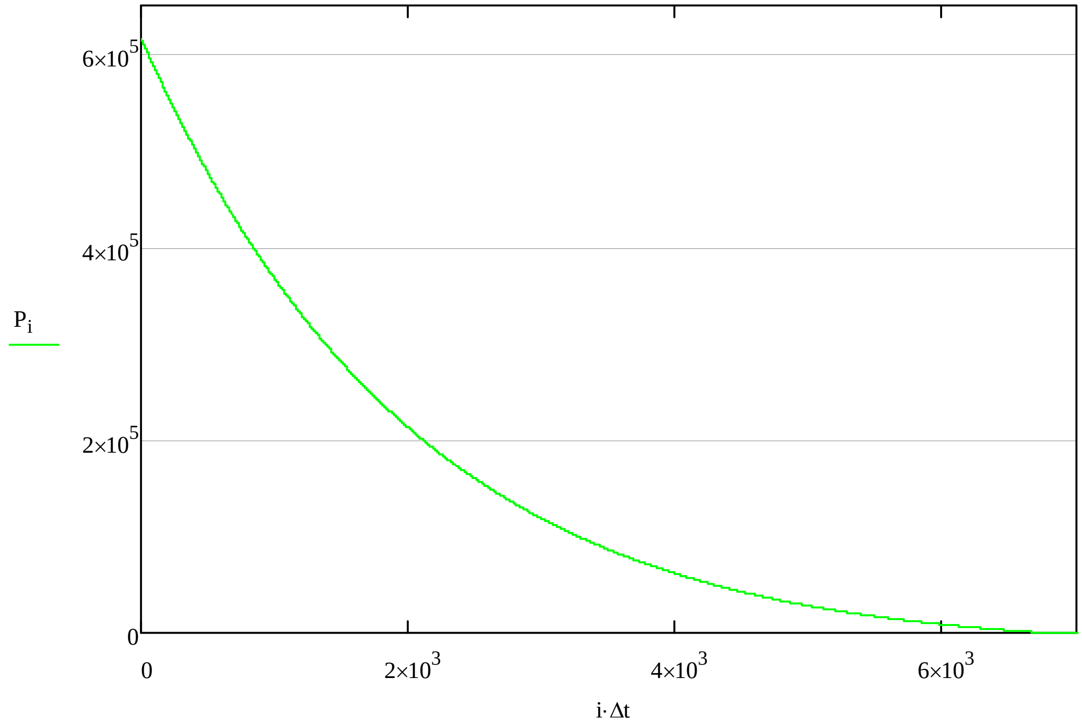

graph: fitting of current [A] versus time [s]

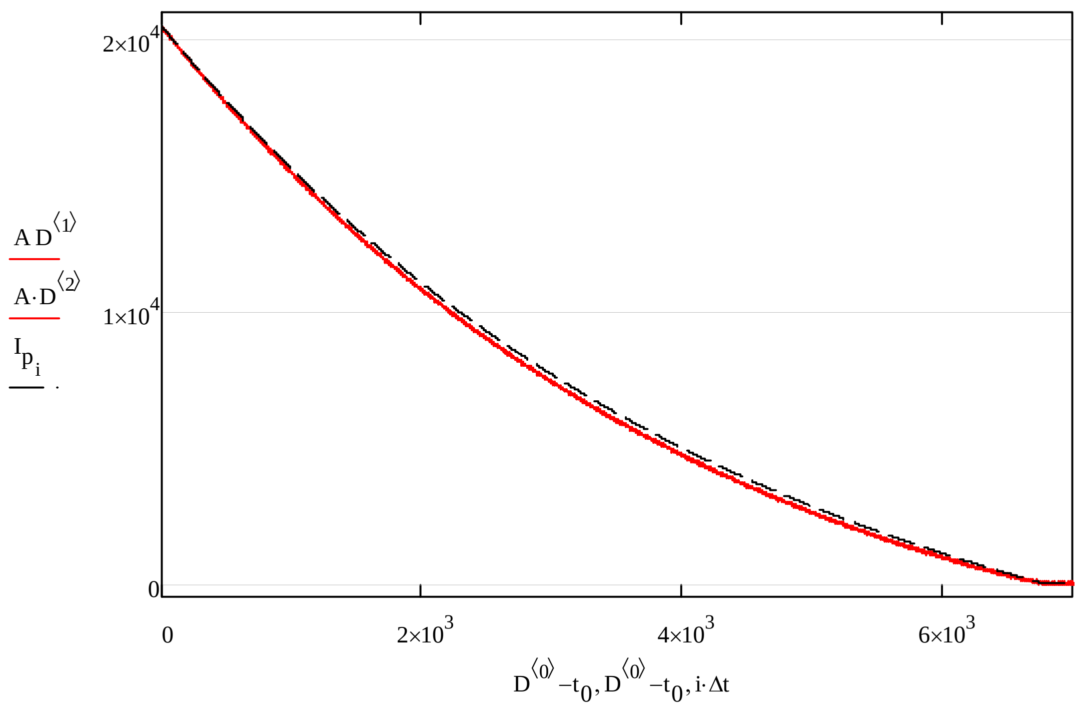

graph: fitting of voltage over coils [V] versus time [s]

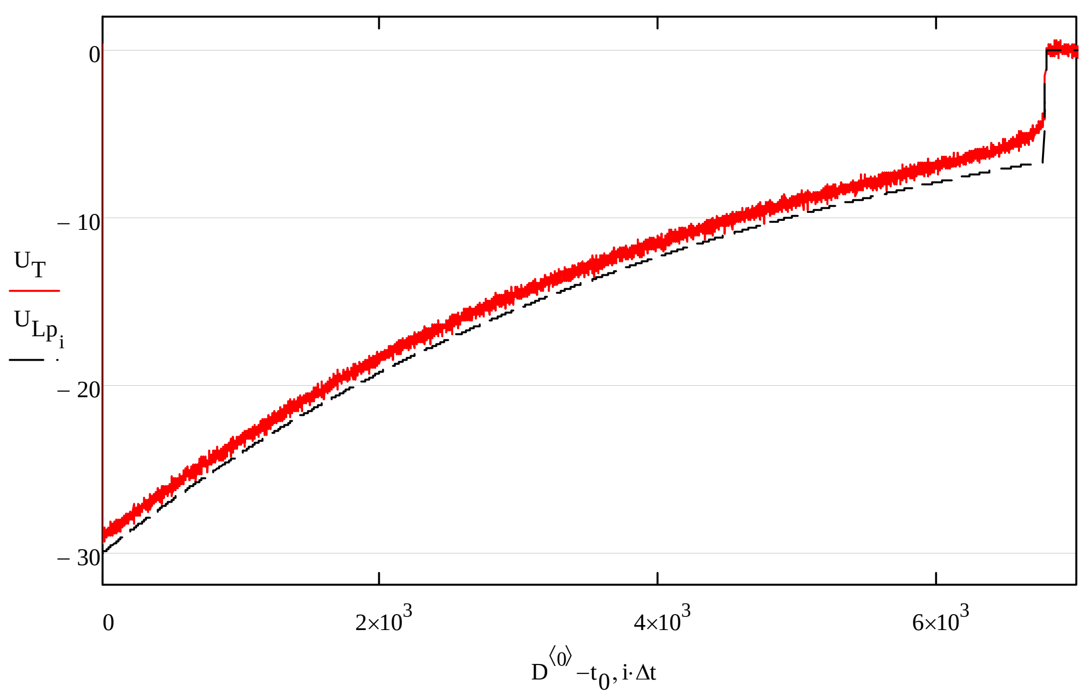

C Simulation of eight coils

calculation properties

number of measurements [-]	$\tau := 32500$		
time between 2 measurements [s]	$\Delta t := 0.2$		
total time of measeurement [s]	$\tau \cdot \Delta t = 6500$	counter	$i := 0..\tau$
number of coils [-]	$N := 8$	counter	$n := 1..N$

coil properties

	primary coils	secondary coils	mutual
resistance [Ω]	$R_p := 1.172 \cdot 10^{-3}$	$R_n :=$	
		$14.52 \cdot 10^{-6}$	
		$13.79 \cdot 10^{-6}$	
		$14.32 \cdot 10^{-6}$	
		$13.67 \cdot 10^{-6}$	
		$13.94 \cdot 10^{-6}$	
		$13.84 \cdot 10^{-6}$	
		$13.80 \cdot 10^{-6}$	
		$14.28 \cdot 10^{-6}$	
inductance [H]	$L_{p_n} :=$	$L_{s_n} :=$	$M_n :=$
	0.6427	$52 \cdot 10^{-6}$	$5.5 \cdot 10^{-3}$
	0.6427	$52 \cdot 10^{-6}$	$5.5 \cdot 10^{-3}$
	0.6427	$52 \cdot 10^{-6}$	$5.5 \cdot 10^{-3}$
	0.6427	$52 \cdot 10^{-6}$	$5.5 \cdot 10^{-3}$
	0.6427	$52 \cdot 10^{-6}$	$5.5 \cdot 10^{-3}$
	0.6427	$52 \cdot 10^{-6}$	$5.5 \cdot 10^{-3}$
	0.6427	$52 \cdot 10^{-6}$	$5.5 \cdot 10^{-3}$
	0.6427	$52 \cdot 10^{-6}$	$5.5 \cdot 10^{-3}$

measurement file

$D :=$

	0	1	2	3	4
0	1	$7.485\cdot10^3$	$7.488\cdot10^3$	-11.915	21.063
1	2	$7.5\cdot10^3$	$7.501\cdot10^3$	6.395	-5.807
2	3	$7.486\cdot10^3$	$7.478\cdot10^3$	-9.475	...

factor current [-] $A := 2.4$

factor voltage [-] $V := \frac{1}{1000}\cdot 1$

start time [s] $t_0 := 671$

voltages coils [V] $U_n := V\cdot\left(D^{\langle 2\cdot n+1\rangle} + D^{\langle 2\cdot n+2\rangle}\right)$

average voltage coils [V] $U_A := \frac{1}{N}\cdot\sum_n U_n$

voltage bridges [V]

$$C_1 := \frac{V\cdot\left(D^{\langle 7\rangle} + D^{\langle 15\rangle} + D^{\langle 11\rangle} + D^{\langle 3\rangle} + D^{\langle 4\rangle} + D^{\langle 12\rangle} + D^{\langle 16\rangle} + D^{\langle 8\rangle}\right) - \frac{8\cdot U_A}{2}}{2} - \frac{V\cdot\left(D^{\langle 18\rangle} + D^{\langle 14\rangle} + D^{\langle 10\rangle} + D^{\langle 6\rangle} + D^{\langle 5\rangle} + D^{\langle 9\rangle} + D^{\langle 13\rangle} + D^{\langle 17\rangle}\right) - \frac{8\cdot U_A}{2}}{2}$$

$$C_2 := \frac{V\cdot\left(D^{\langle 7\rangle} + D^{\langle 15\rangle} + D^{\langle 11\rangle} + D^{\langle 3\rangle}\right) - \frac{4\cdot U_A}{2}}{1} - \frac{V\cdot\left(D^{\langle 4\rangle} + D^{\langle 12\rangle} + D^{\langle 16\rangle} + D^{\langle 8\rangle} + D^{\langle 18\rangle} + D^{\langle 14\rangle} + D^{\langle 10\rangle} + D^{\langle 6\rangle} + D^{\langle 5\rangle} + D^{\langle 9\rangle} + D^{\langle 13\rangle} + D^{\langle 17\rangle}\right) - \frac{12\cdot U_A}{2}}{3}$$

$$C_3 := \frac{V\cdot\left(D^{\langle 5\rangle} + D^{\langle 9\rangle} + D^{\langle 13\rangle} + D^{\langle 17\rangle}\right) - \frac{4\cdot U_A}{2}}{1} - \frac{V\cdot\left(D^{\langle 7\rangle} + D^{\langle 15\rangle} + D^{\langle 11\rangle} + D^{\langle 3\rangle} + D^{\langle 4\rangle} + D^{\langle 12\rangle} + D^{\langle 16\rangle} + D^{\langle 8\rangle} + D^{\langle 18\rangle} + D^{\langle 14\rangle} + D^{\langle 10\rangle} + D^{\langle 6\rangle}\right) - \frac{12\cdot U_A}{2}}{3}$$

initial values

voltage diode [V]

current primary coil [A]

current secondary coil [A]

$$\begin{pmatrix} U_{d_0} \\ I_{p_0} \\ I_{s_{0,n}} \end{pmatrix} := \begin{pmatrix} 10\cdot 0.665 \\ A\cdot 7490 \\ 0 \end{pmatrix}$$

calculation of all values

$$\begin{pmatrix} U_{d_{i+1}} \\ I_{p_{i+1}} \\ I_{s_{i+1,n}} \end{pmatrix} := \begin{bmatrix} \text{if}\left[\left[I_{p_i} + \dfrac{-R_p \cdot I_{p_i} + \sum_n \left(\dfrac{M_n \cdot R_n}{L_{s_n}} \cdot I_{s_{i,n}}\right) - U_{d_0}}{\sum_n \left(L_{p_n}\right) - \sum_n \left[\dfrac{\left(M_n\right)^2}{L_{s_n}}\right]} \cdot \Delta t\right] \le 0, \sum_n \left(\dfrac{M_n \cdot R_n}{L_{s_n}} \cdot I_{s_{i,n}}\right), U_{d_0}\right] \\ \text{if}\left[\left[I_{p_i} + \dfrac{-R_p \cdot I_{p_i} + \sum_n \left(\dfrac{M_n \cdot R_n}{L_{s_n}} \cdot I_{s_{i,n}}\right) - U_{d_i}}{\sum_n \left(L_{p_n}\right) - \sum_n \left[\dfrac{\left(M_n\right)^2}{L_{s_n}}\right]} \cdot \Delta t\right] \le 0, 0, \left[I_{p_i} + \dfrac{-R_p \cdot I_{p_i} + \sum_n \left(\dfrac{M_n \cdot R_n}{L_{s_n}} \cdot I_{s_{i,n}}\right) - U_{d_i}}{\sum_n \left(L_{p_n}\right) - \sum_n \left[\dfrac{\left(M_n\right)^2}{L_{s_n}}\right]} \cdot \Delta t\right]\right] \\ I_{s_{i,n}} + \left[-\dfrac{R_n}{L_{s_n}} \cdot I_{s_{i,n}} + \dfrac{M_n}{L_{s_n}} \cdot \dfrac{R_p \cdot I_{p_i} - \sum_n \left(\dfrac{M_n \cdot R_n}{L_{s_n}} \cdot I_{s_{i,n}}\right) + U_{d_i}}{\sum_n \left(L_{p_n}\right) - \sum_n \left[\dfrac{\left(M_n\right)^2}{L_{s_n}}\right]}\right] \cdot \Delta t \end{bmatrix}$$

	primary coil	secondary coil
voltage resistance [V]	$U_{Rp_i} := R_p \cdot I_{p_i}$	$U_{Rs_{i,n}} := R_n \cdot I_{s_{i,n}}$
voltage coil [V]	$U_{Lp_{i,n}} := L_{p_n} \cdot \dfrac{I_{p_{i+1}} - I_{p_i}}{\Delta t} + M_n \cdot \dfrac{I_{s_{i+1,n}} - I_{s_{i,n}}}{\Delta t}$	$U_{Ls_{i,n}} := L_{s_n} \cdot \dfrac{I_{s_{i+1,n}} - I_{s_{i+1,n}}}{\Delta t} + M_n \cdot \dfrac{I_{p_{i+1}} - I_{p_i}}{\Delta t}$

average voltage coils [V] $\quad U_{LpA_i} := \dfrac{1}{N} \cdot \sum_n U_{Lp_{i,n}}$

Bridge 1 (2-2): $\quad B_{1_i} := \dfrac{2 \cdot \left(U_{Lp_{i,3}} + U_{Lp_{i,7}} + U_{Lp_{i,5}} + U_{Lp_{i,1}} - 4 \cdot U_{LpA_i}\right)}{2 \cdot 2} - \dfrac{2 \cdot \left(U_{Lp_{i,8}} + U_{Lp_{i,6}} + U_{Lp_{i,4}} + U_{Lp_{i,2}} - 4 \cdot U_{LpA_i}\right)}{2 \cdot 2}$

Brigde 2 (1-3 +): $\quad B_{2_i} := \dfrac{U_{Lp_{i,3}} + U_{Lp_{i,7}} + U_{Lp_{i,5}} + U_{Lp_{i,1}} - 4 \cdot U_{LpA_i}}{2 \cdot 1} - \dfrac{U_{Lp_{i,3}} + U_{Lp_{i,7}} + U_{Lp_{i,5}} + U_{Lp_{i,1}} + 2 \cdot \left(U_{Lp_{i,8}} + U_{Lp_{i,6}} + U_{Lp_{i,4}} + U_{Lp_{i,2}}\right) - 12 \cdot U_{LpA_i}}{2 \cdot 3}$

Bridge 3 (1-3 -): $\quad B_{3_i} := \dfrac{U_{Lp_{i,8}} + U_{Lp_{i,6}} + U_{Lp_{i,4}} + U_{Lp_{i,2}} - 4 \cdot U_{LpA_i}}{2 \cdot 1} - \dfrac{U_{Lp_{i,8}} + U_{Lp_{i,6}} + U_{Lp_{i,4}} + U_{Lp_{i,2}} + 2 \cdot \left(U_{Lp_{i,3}} + U_{Lp_{i,7}} + U_{Lp_{i,5}} + U_{Lp_{i,1}}\right) - 12 \cdot U_{LpA_i}}{2 \cdot 3}$

graph: primary and secondary currents [A] versus time [s]

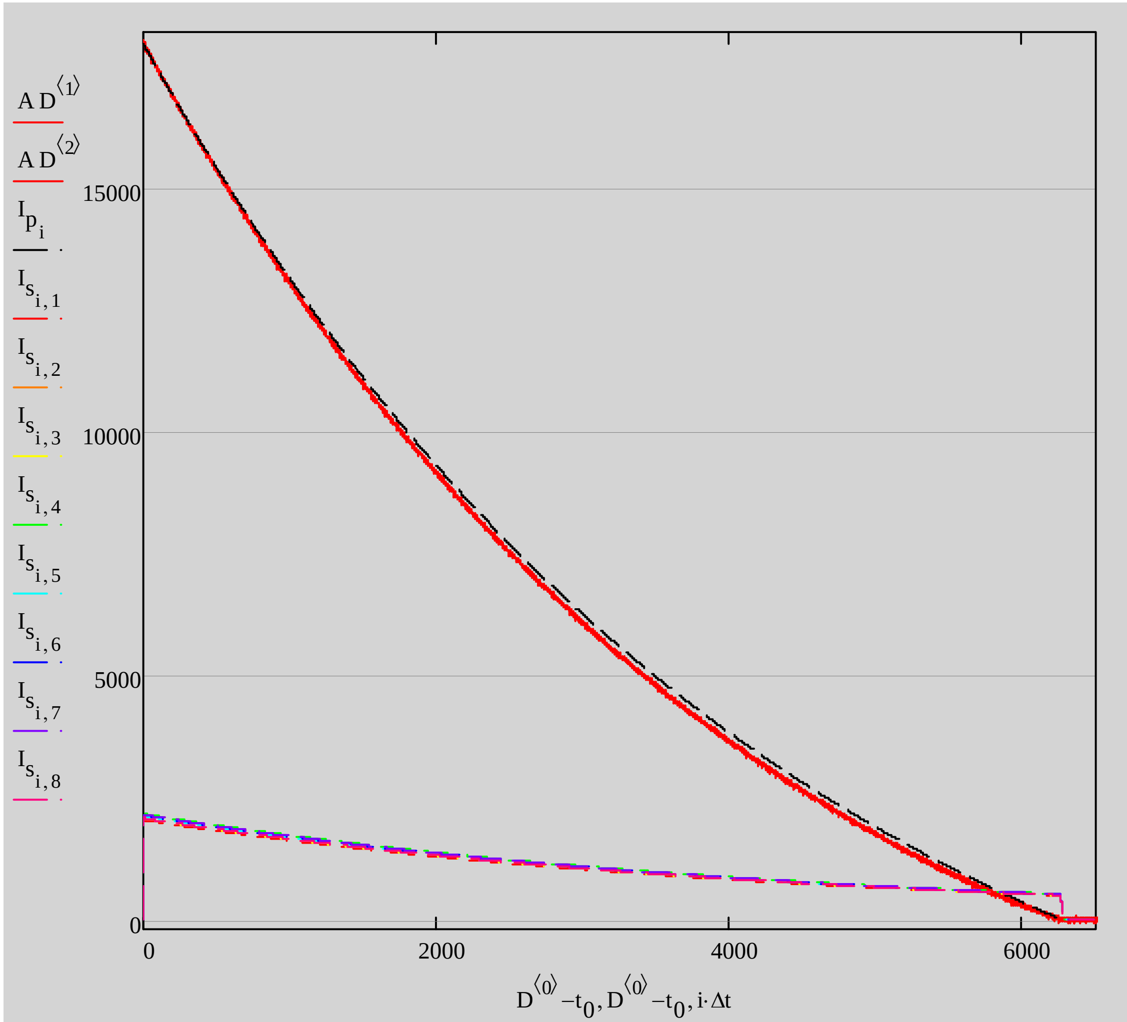

graph: average voltage over a primary coil [V] versus time [s]

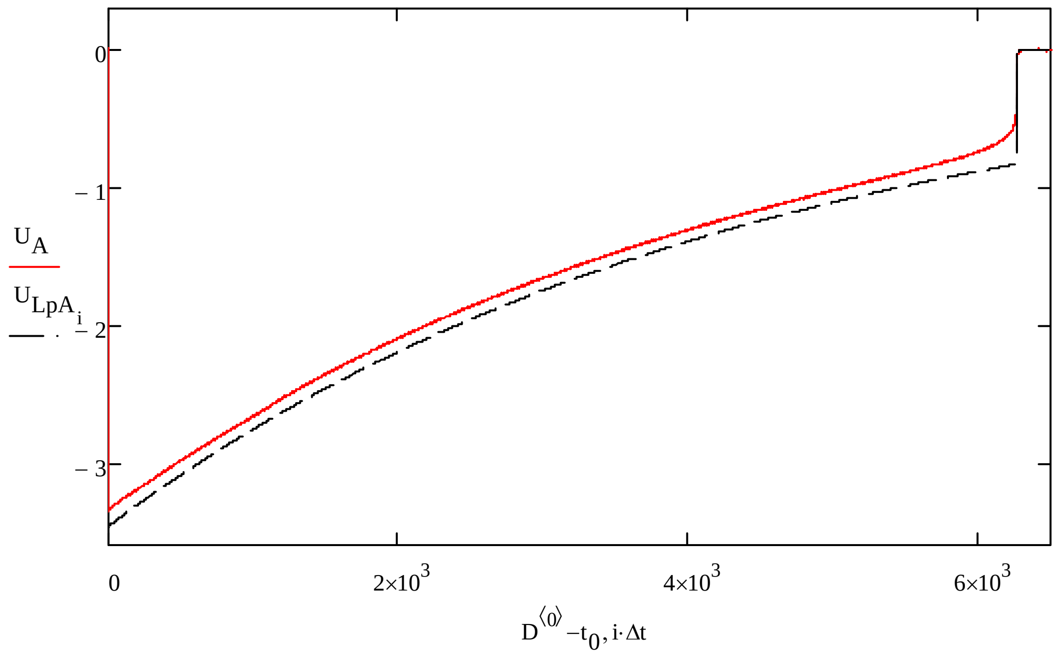

graphs: bridge voltages [V] versus time [s]

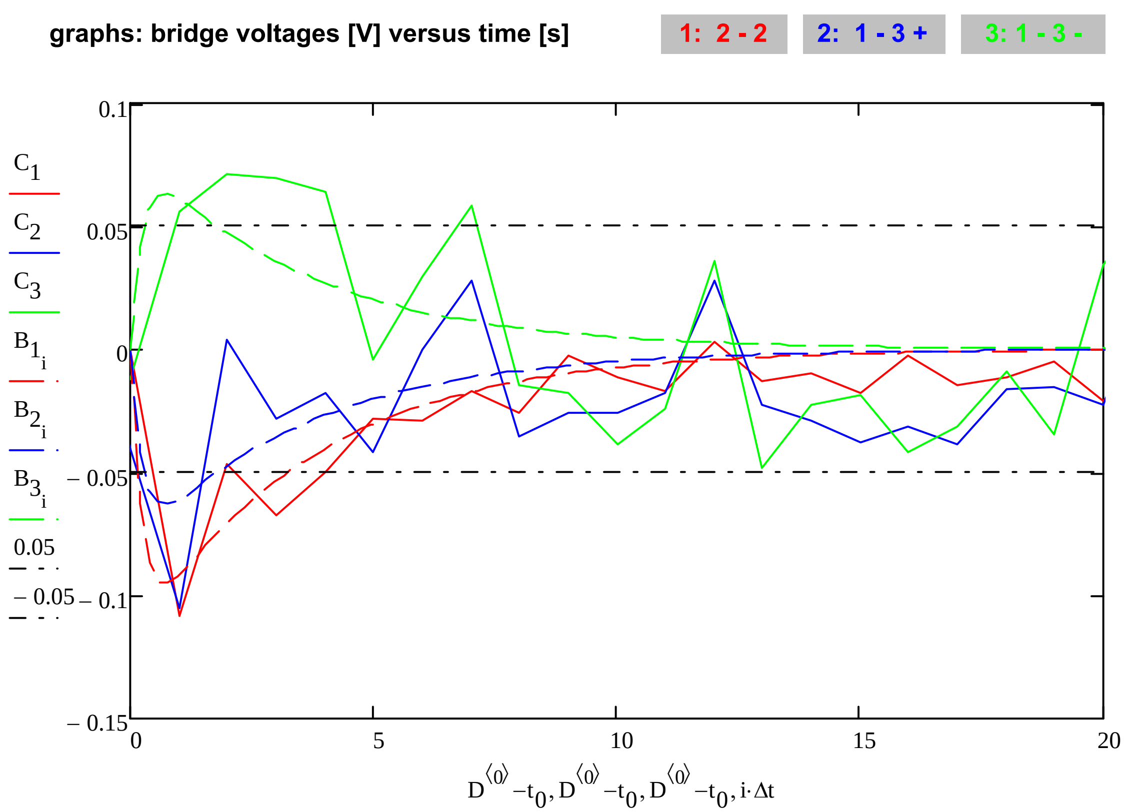

graph: voltages over each primary coils [V] versus time [s]

$c := 0.120$

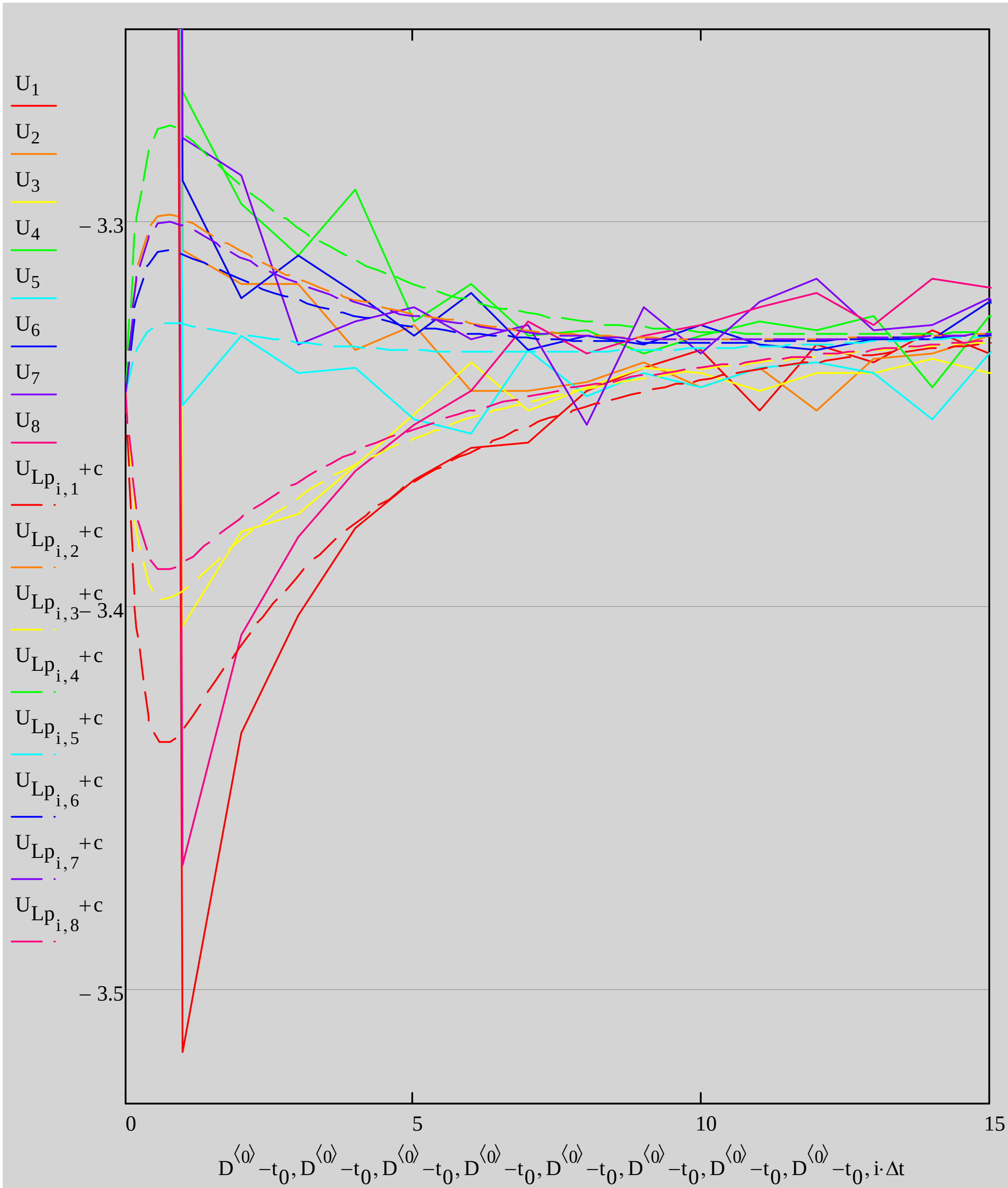

D Editing of data of fast dump

For the calculations of the energy distribution during the fast dump, the resistance of the superconductor is needed. With a program, the measured data is filtered.

When in this report is referred to a Smooth-function, then this is averaging of the signal. When this smooth function is used, one has to define a variable. This function with 5 as value for the variable means that the function will be averaged over 5 points.

The data of the fast dump is from measurements 100 times per second. When the Smooth-function is used with the value 1000, it means that an average will be taken over a period of 10 seconds.

When a graph is given, the program can also differentiate and integrate the graph.

In the formulas underneath is shown how the measured data is always edited (if mentioned). There is also an example plot shown, which comes from the measurement of the BT at 20.5kA.

- $\textit{Measured current} \xrightarrow{\textit{Smooth}\,1000} \textit{Smoothed current}$
  (Graph does not show whole measurement, SI = smoothed current)

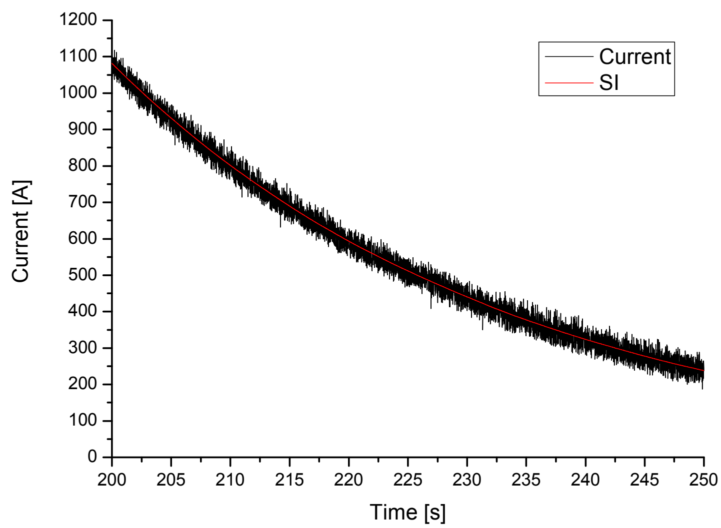

- $\frac{d}{dt}(\textit{Smoothed current}) \xrightarrow{\textit{Smooth}\,1200} \textit{Smoothed derivative of current}$
  (Graph does not show whole measurement, SI = smoothed current, SdI/dt = smoothed derivative of current)

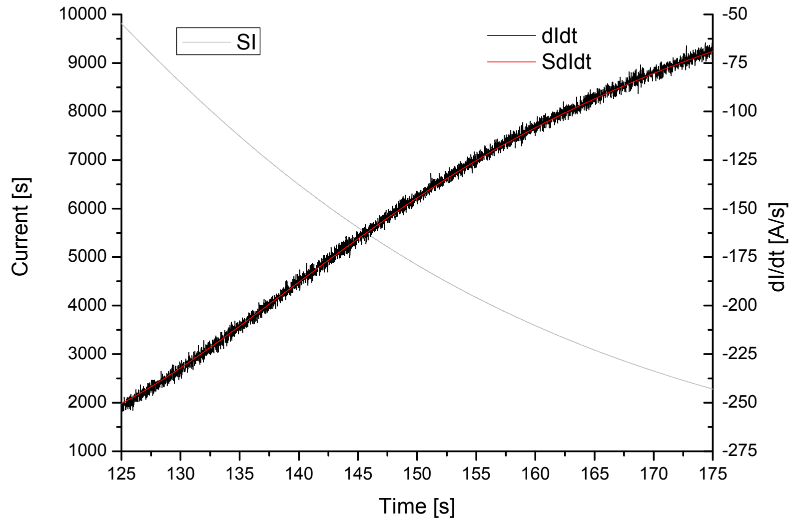

- $Measured\ voltage \xrightarrow{Smooth\ 500} Smoothed\ voltage$

  (Graph shows whole measurement, 1x12 = measured voltage of one double pancake, S1x12 = smoothed voltage)

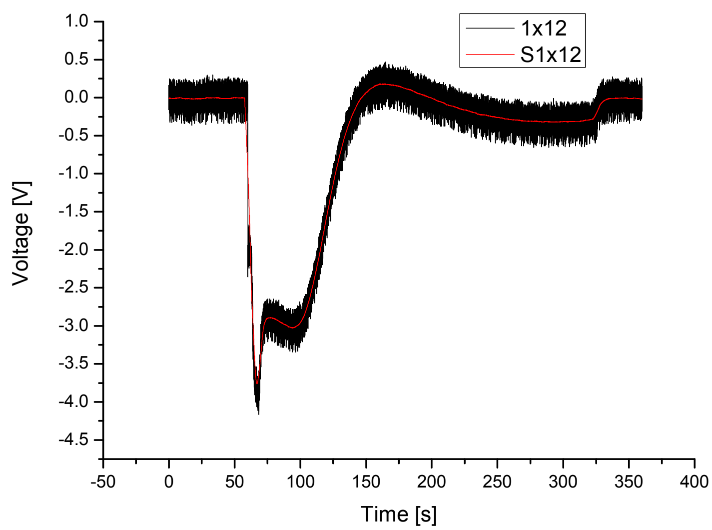

E Material properties

E.1 Aluminium

Conditions: RRR = 1500, B = 1T
Density: 2698 kg/m^3
Resistivity:

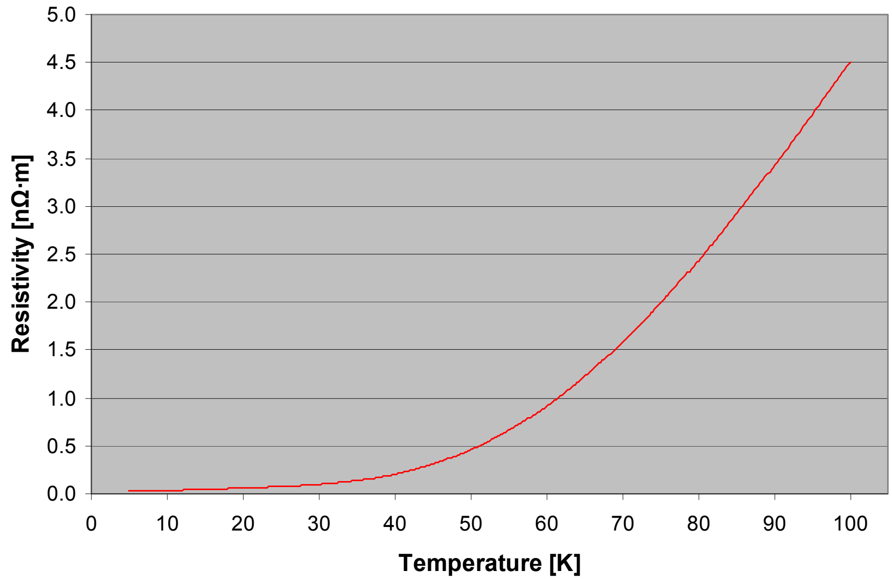

Enthalpy (temperature = 5K → enthalpy = 0)

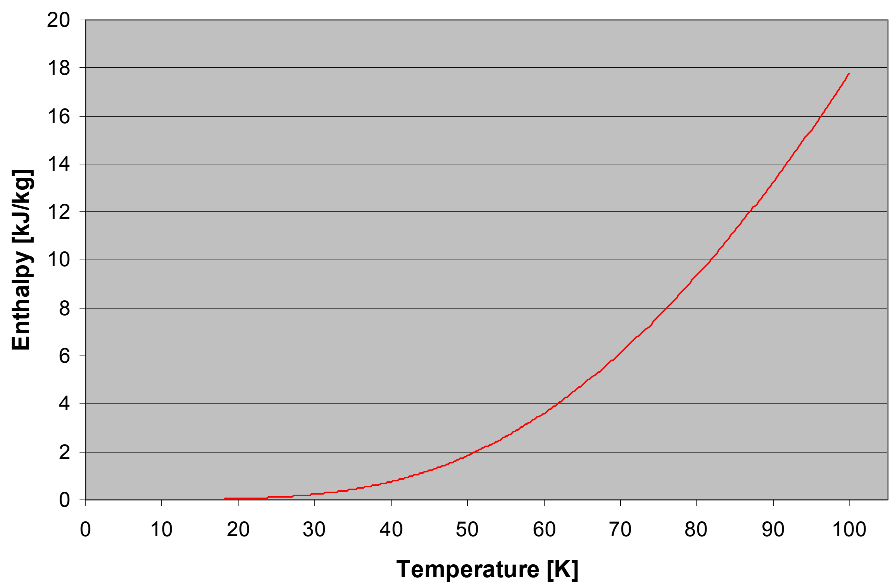

E.2 Copper

Conditions: RRR = 1500, B = 1T
Density: 8960 kg/m^3
Enthalpy (temperature = 5K → enthalpy = 0):

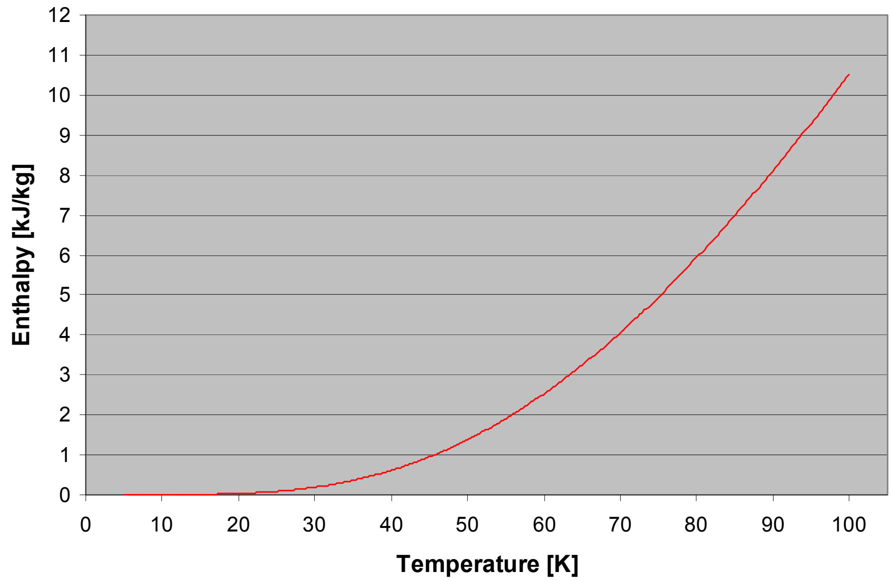

E.3 Insulation (Fiberglas-epoxy G-10)

Density: 1948 kg/m^3
Enthalpy (temperature = 5K → enthalpy = 0):